U. S. DEPARTMENT OF COMMERCE
Luther H. Hodges, Secretary
WEATHER BUREAU
Robert M. White, Chief

NATIONAL SEVERE STORMS PROJECT

REPORT NO. 21

On the Motion and Predictability of Convective Systems

As Related to the Upper Winds In a Case of Small Turning of Wind With Height.

by

James C. Fankhauser

National Severe Storms Project, Kansas City, Mo.

Washington, D. C.
January 1964

CONTENTS

ON THE MOTION AND PREDICTABILITY OF CONVECTIVE SYSTEMS AS RELATED TO THE UPPER WINDS IN A CASE OF SMALL TURNING OF WIND WITH HEIGHT

James C. Fankhauser
National Severe Storms Project
Kansas City, Missouri [1]

ABSTRACT

Radar composites of the extensive squall-line development of May 28, 1962, as well as the individual convective storms comprising the line, are compared to the mean wind in the troposphere. The case is distinctive since, contrary to the situation most common to vigorous convective outbreaks, there is only small turning of wind with height. The component contributions of translation and propagation toward echo motion are proposed to be linked to the mean and shear winds. Their influences on the motion of individual elements as well as on the aggregate line are discussed and the relationship between movements of individual storms and the squall line as a whole are summarized. Squall-line displacement and orientation are found to have a high degree of correlation with mean wind direction. Study of the movements of propagating echo complexes within the range of WSR-57 radar located at Oklahoma City discloses a great degree of persistence in storm direction and speed when a particular echo is considered, even though there is appreciable variation between different storms within a relatively small area under the influence of a uniform mean wind field. Storm paths are nearly symmetrically distributed about the mean wind with a standard deviation from mean wind direction of 9 degrees to the right and left. Echo speed is found to be on the average in excess of the layer mean wind speed.

On the basis of the statistical scatter in storm behavior for this special case, a technique for assessing the vulnerability, with respect to thunderstorm passage, of a point lying downstream from an existing storm echo is presented through the application of probability theory.

1. INTRODUCTION

The processes relevant to the larger-scale environment common to the development of convective storms have become increasingly well known in recent years [1]. Since the general area of convective outbreak can be linked to the broad-scale circulations, there should be some relationship between macroscale circulation and the motion of convective storms.

---

[1] Present affiliation, National Severe Storms Laboratory, Norman, Okla.; temporarily assigned to the National Center for Atmospheric Research, Boulder, Colorado.

Statement of problem. The purpose of this report is to compare the motion of individual storms within the extensive squall-line development of May 28, 1962, to the upper winds and to assess qualitatively the contributions of the motions of individual storms to the displacement of the squall-line system as a whole. Only after generalized appraisals of the relationships between environment circulation and thunderstorm motion have been obtained for varying upper-wind conditions can we hope to approach the problem of accurately predicting thunderstorm movement from the standpoint of winds aloft. A distinctive feature prompting the selection of this case was the unusually small degree of wind turning with height (see figs. 1 and 2). The predictability of the motion of individual storms in this special case will be approached through the application of probabilities.

Brief historical review. Many studies have been made of the relation between the movement of precipitation areas as depicted by radar and the winds at some particular level or within various tropospheric layers [3,5,7,9,10,13,14]. Most of the correlations of storm movements with winds at a particular level (most frequently 700 mb. or 10,000 ft.) have been high when storms were nonpropagating and their size was small and uniform. High correlations are less common, however, when propagating cumulonimbi of varying sizes are considered.

Humphreys [11] states, "The velocity of the thunderstorm is nearly the velocity of the atmosphere in which the bulk of the cloud is located." This is in agreement with findings of the Thunderstorm Project [7], although with strong winds there was a tendency for storms to move somewhat more slowly than the mean speed of the cloud-bearing layer.

As mentioned above, the case dealt with here is characterized by small change of wind direction with height. There is increasing empirical evidence that in cases of appreciable vertical veering of wind (the situation most common to vigorous convective activity) large storms tend to deviate to the right of the upper winds [6,20]. A separate report will deal with the motions of storms in wind situations of this type.

2. WIND FIELDS IN CONVECTIVE SITUATIONS

Disturbed character of upper winds. The most serious problem in dealing with the convective storm-steering flow problem is the selection of a representative wind field. Upper-air soundings made during the passage of, or in the vicinity of, thunderstorms are usually unrepresentative of the atmosphere in which the storms are embedded. Wind observations in particular are locally disturbed by the vigorous updrafts and downdrafts within the thunderstorms themselves. The magnitude of the divergence related to these localized vertical motions may be as much as two orders greater than for the synoptic scale and may extend for tens of miles on either side of a large and active

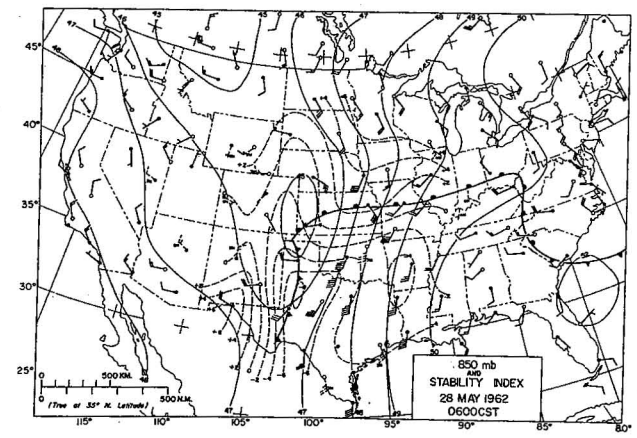

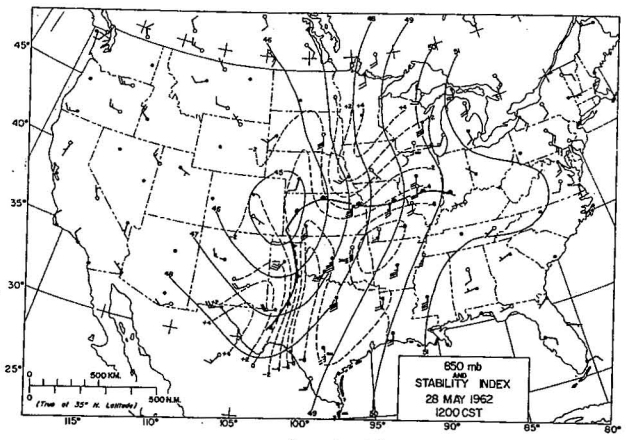

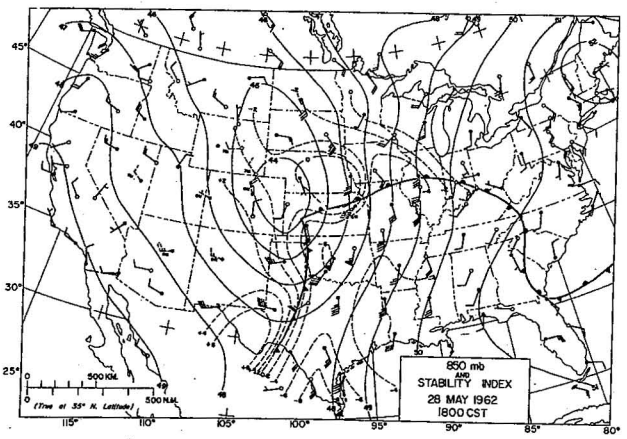

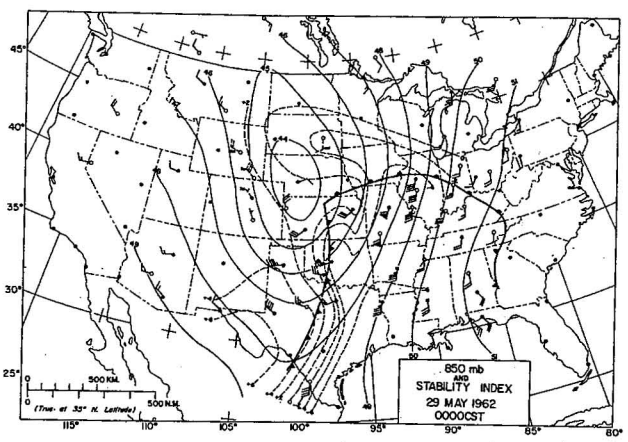

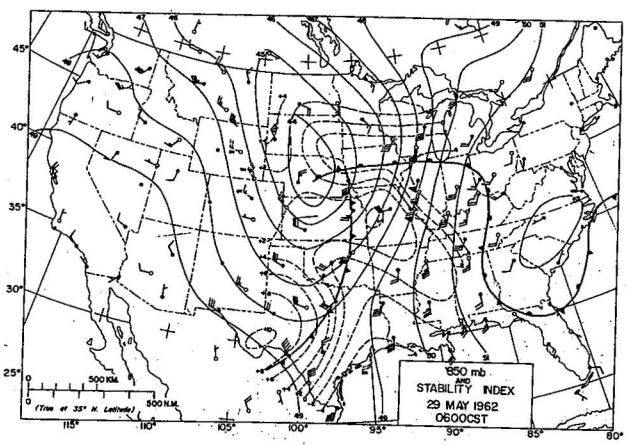

Figure 1.— 850-mb. contour and stability analysis, May 28-29, 1962. Solid lines are height contours in hundreds of feet. Dashed lines are isolines of stability index at 2°C. intervals.

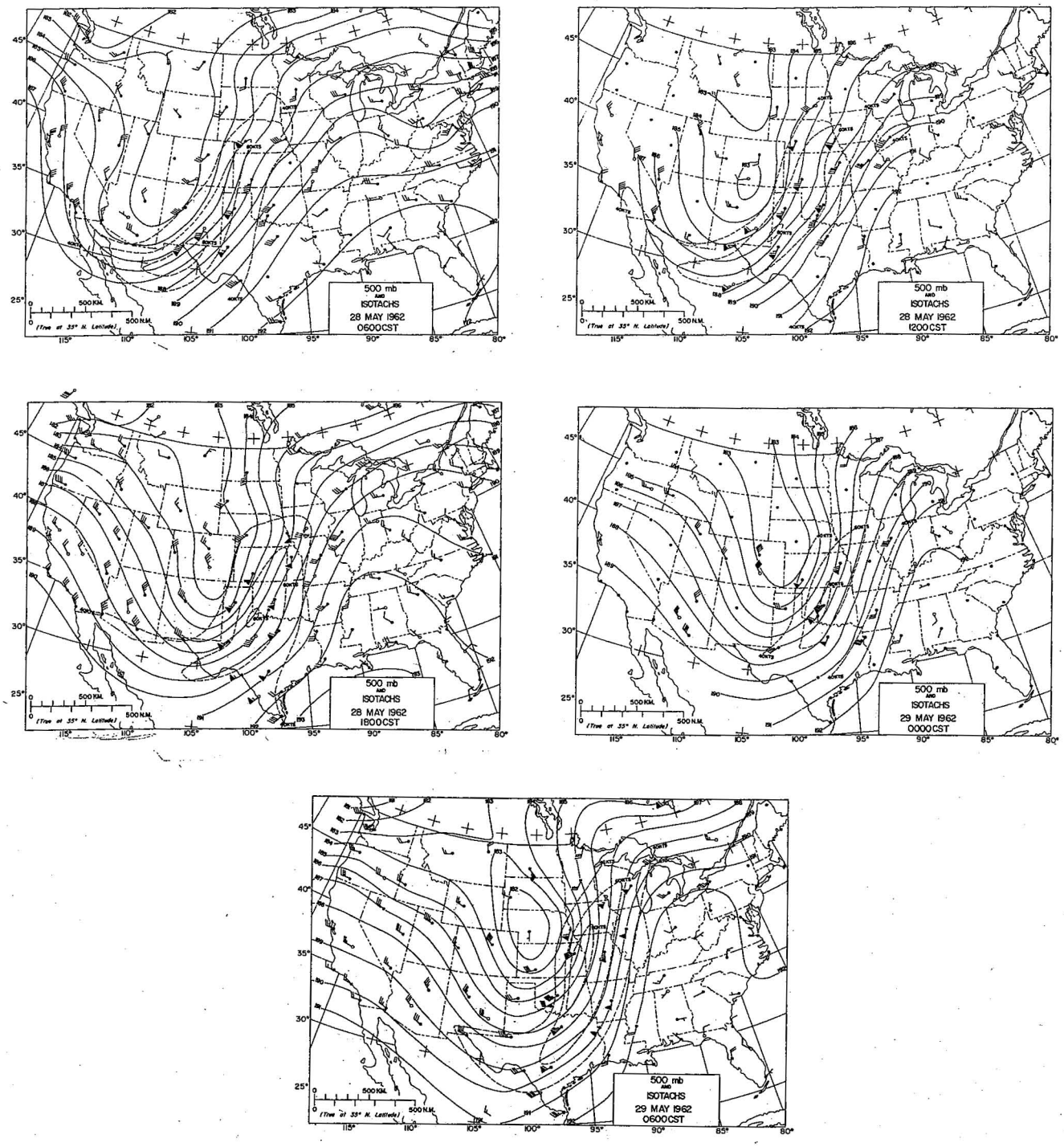

Figure 2.— 500-mb. contour and isotach and analysis, May 28-29, 1962. Solid lines are contours in hundreds of feet. Dashed lines are isotachs at 20 kt. intervals.

convective system. This disturbance of the wind field is typified by exaggerated net, low-level horizontal convergence and upper-level divergence.

The influence of convective activity on proximity upper-wind observations is illustrated by figures 3(a) and (b). Serial soundings made at 90-min., 3-hr., and 6-hr. intervals about map time have been adjusted in time and space and placed relative to the squall line with respect to its mean movement. The systematic veering of the wind in lower levels and backing in upper levels are consistent features at individual stations over which the squall line passes. Sharp changes in vector velocity are also evident in time at individual stations and in space between stations with nearly the same relative position to the squall line.

Selection of meaningful wind. Since the mean divergence through the depth of a cloud system must be nearly zero, it is suggested that the effects of large divergence and convergence in individual layers may be overcome by considering the mean wind through the entire cloud-bearing layer.

The mean winds at individual stations throughout the central United States were computed graphically by applying the equation:

$$\mathbb{V} = \frac{\mathbb{V}_{850} + \mathbb{V}_{700} + \mathbb{V}_{500} + \mathbb{V}_{300}}{4}$$

The winds at the various levels were taken to be representative of the layers 800-900, 600-800, 400-600, and 200-400 mb. The mean wind in the troposphere up to 200 mb. can be considered representative of the cloud-bearing layer since typical Great Plains convective storms usually extend to about 40,000 ft. average height. Although the lowest of the above layers is given equal weight despite its smaller mass thickness, this is probably to some extent justified since such a high proportion of air drawn into a thunderstorm originates at the low levels.

Interpolation between regular observation times, supplemented by PIBALS and special rawinsonde releases, made it possible to prepare intermediate mean wind fields at 28/1200 CST, 28/1500 CST, and 29/0000 CST. A synoptic sequence of the mean wind field was then available from 28/0600 CST through 29/0600 CST at intervals of 6-hr. or less. These mean wind fields were analyzed with respect to streamlines, isotachs, and isogons (fig. 4). The 850-300 mb. vector mean wind field for 28/1800 CST is shown in figure 3(c). As expected, the exaggerated disturbances at individual levels are eliminated and relatively smooth streamlines result.

The variations in the isotachs and isogons displayed in figure 4 are characteristic of those of the "cyclone scale," and

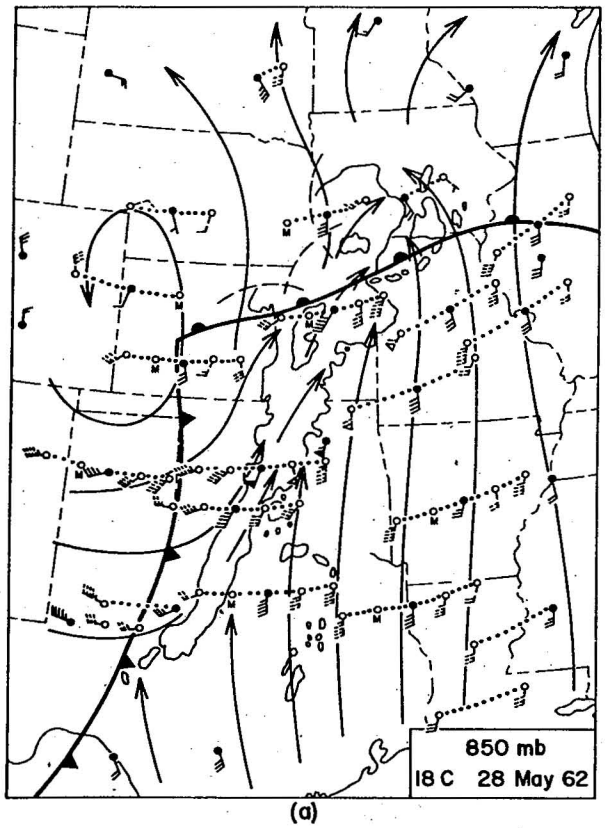

(a)

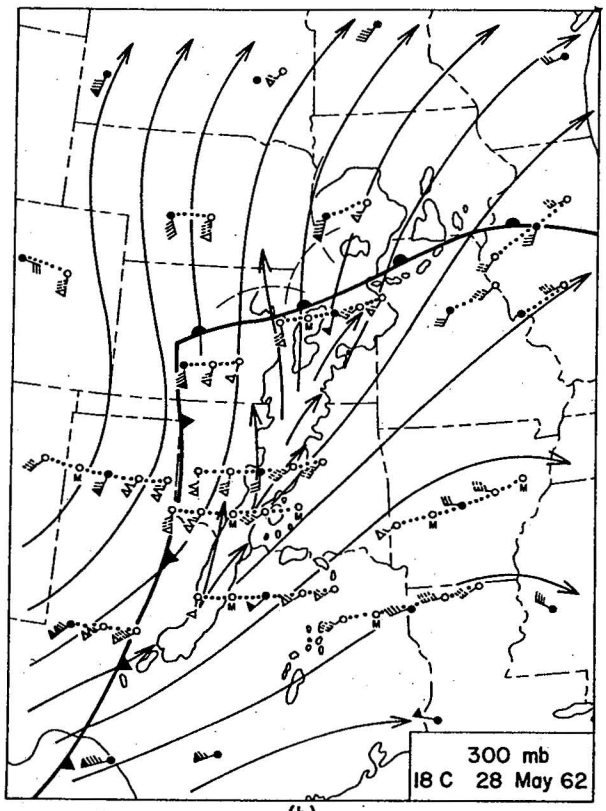

(b)

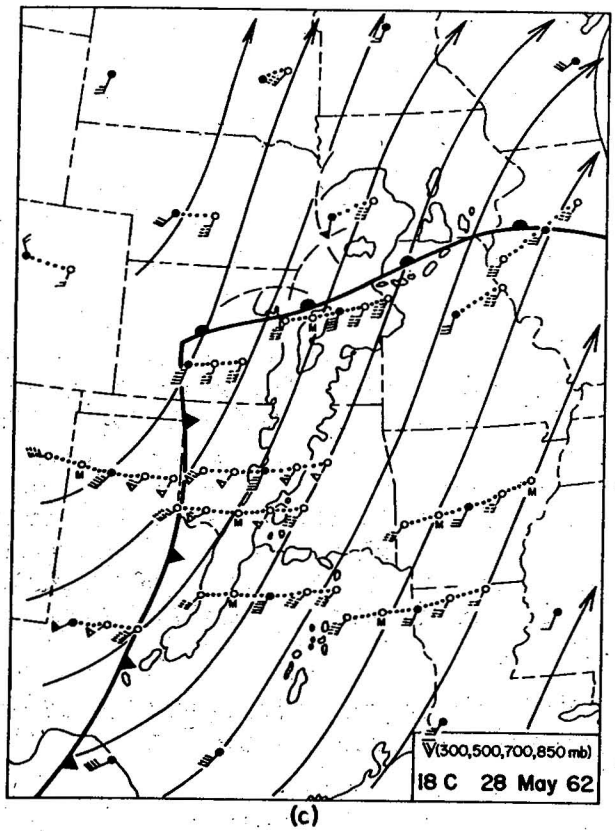

(c)

Figure 3.— Wind fields in the squall-line situation of May 28, 1962. Arrows are streamlines; irregular thin lines are composite radar echoes; heavy lines, surface fronts. Dashed wind symbols are observations 6 hr. (farthest right) and 3 hr. before, and 3 and 6 hr. (left) after 1800 CST, at stations with solid wind symbols at 1800 CST.

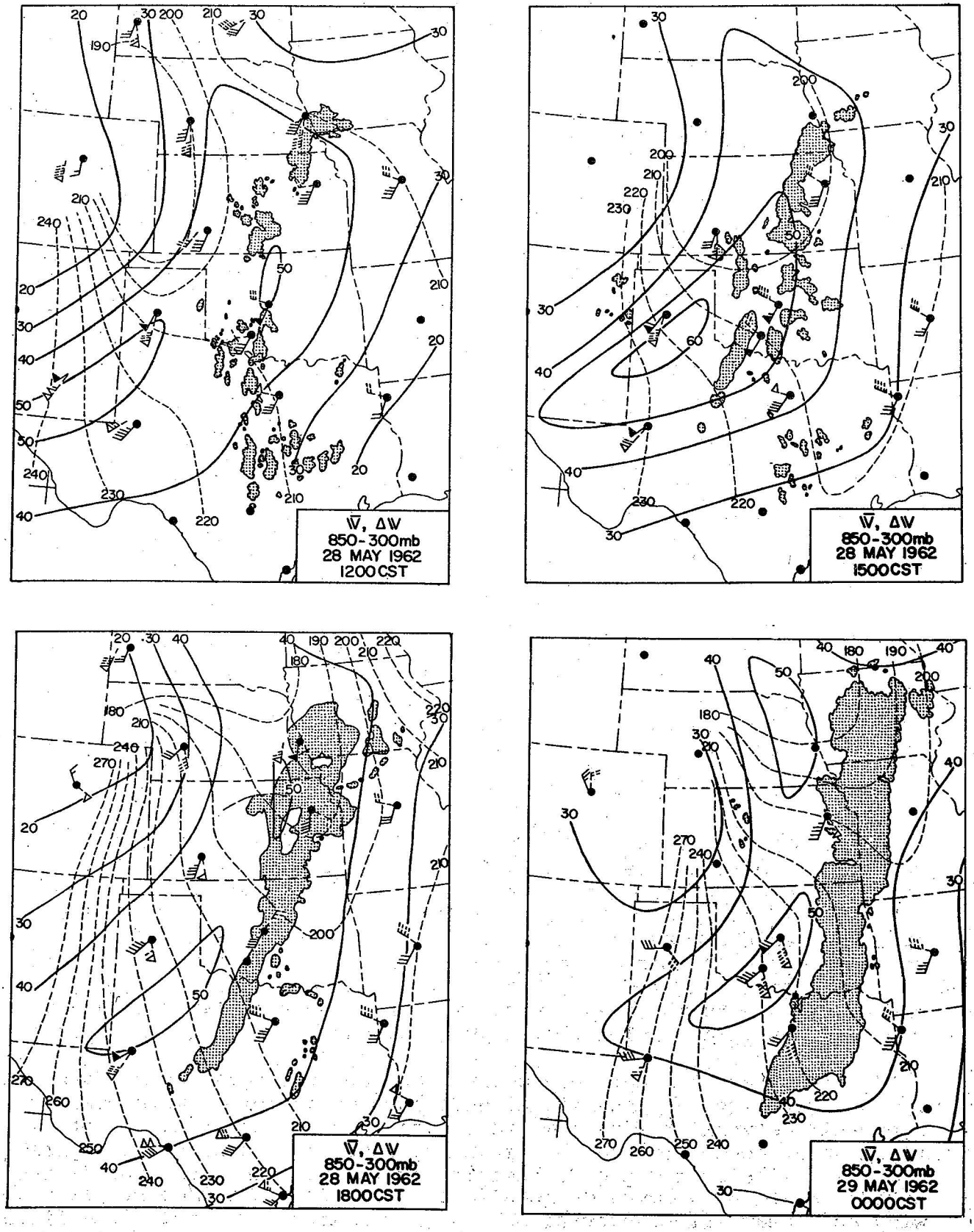

Figure 4.— Mean wind (solid wind symbols) and wind shear (dashed symbols) through 850-300-mb. layer, May 28-29, 1962. Solid lines are mean wind isotachs in knots; dashed lines are isogons in degrees.

individual mean winds that did not correspond to seemingly uniform changes were considered unrepresentatively disturbed and disregarded in the analysis.

3. CHARACTERISTICS OF SQUALL-LINE MOTION

Even before weather radar came into widespread use as a thunderstorm detecting tool, visual observations and time lapse photography [17] led observers to conclude that a part of an individual cloud's motion is achieved by growth and dissipation processes. The present generally accepted terminology for this type of motion is propagation. The remaining portion of individual element motion due to the environment steering flow is generally referred to as translation or advection.

Contributions of translation and propagation. Since the squall line is comprised of a line of individual thunderstorms, the motion of the line may be considered to consist of the two terms, propagation and translation. In the case of the squall line, however, propagation must also include, in addition to new growth on individual storms, the contribution made by the formation of new storms outside of the line which eventually join or become a part of the line. It is important to note that translation alone cannot account for line motion since the average lifetime of individual cells is usually considerably less than that of the line.

The variation in the degree to which translation and propagation contribute to line motion results in short-term irregularities in line speed and orientation. We will substantiate later in this report the findings of previous investigators [5,7] that the contribution of propagation to apparent movement of the squall line becomes large when the actual transport of convective clouds by the environment in the direction of the line is small.

Mean and shear wind contributions toward line motion. Newton and Newton [19] have proposed that the tendency for convective clouds to accelerate toward the velocity of the environment results from the induced pressure fields created by relative cloud and environment air motions. In addition, when the wind veers appreciably with height, there should also be a tendency for a particular line element to drift to the right as a consequence of new growth on its right forward flank. It may be inferred from these arguments that the motion of line components is due to the mean wind in the cloud-bearing layer combined with a propagation linked to the vertical shear.

In order to accurately define the vertical shear over a storm and quantitatively assess its effects on propagation, a much denser upper-air network than is now available would be required. Hypothetical shear conditions can be employed, however, and added to typical mean wind fields to depict schematically the influence on squall-line motion caused by varying degrees in the contributions made by the mean wind and shear effects acting on individual line elements. (See fig.5).

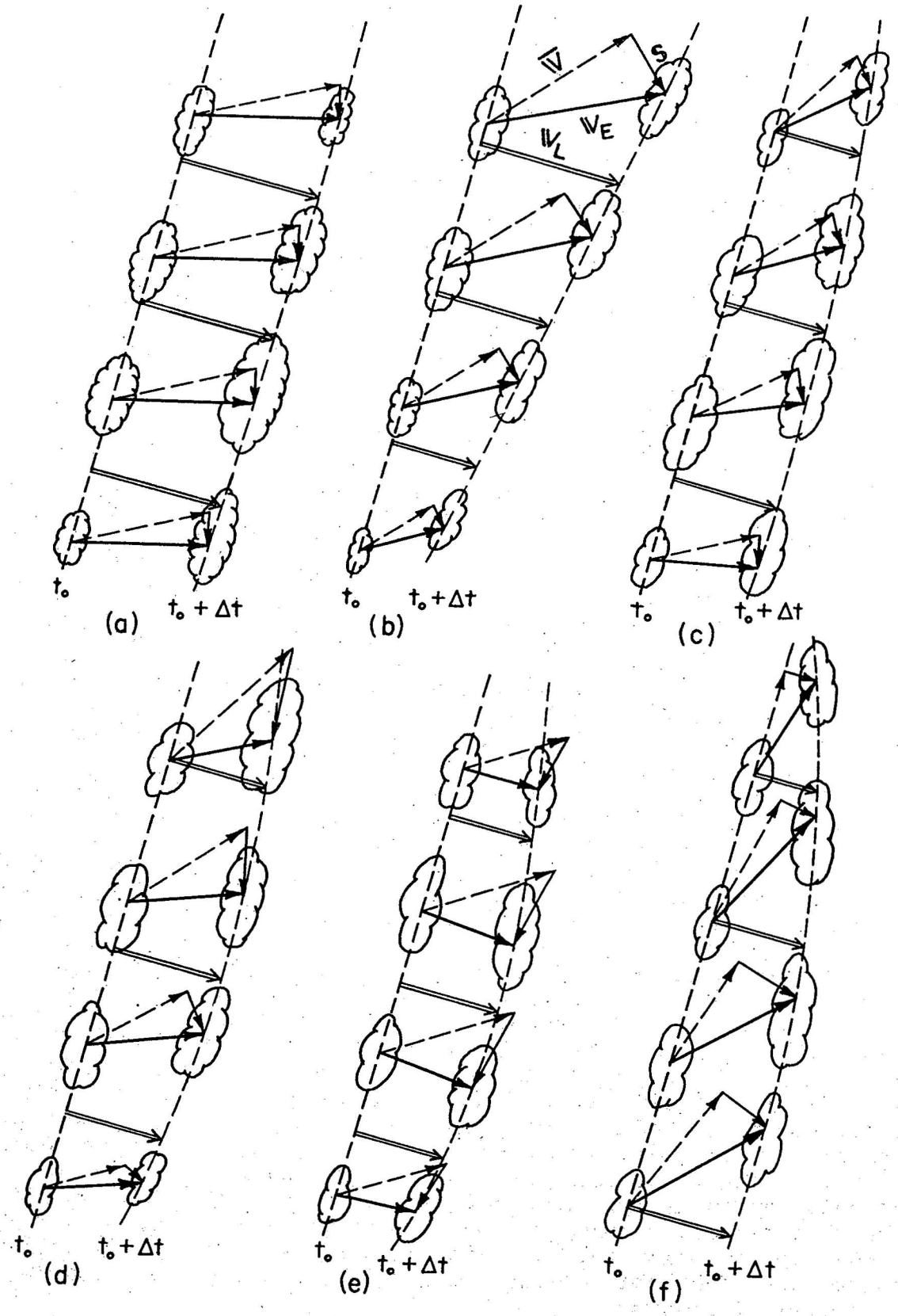

Figure 5.— Schematic presentation of the influence of mean wind and shear component on squall-line motion and orientation. The following vector notation is used: $\mathbb{V}$ = mean wind; $\mathbb{S}$ = shear component; $\mathbb{V}_E$ =individual echo motion; and $\mathbb{V}_L$ = line motion.

Figure 5(a) is an example of uniform line displacement when both the mean wind ($\overline{\mathbb{V}}$) and the shear component ($) are constant along the squall-line zone. In figure 5(b), $|\overline{\mathbb{V}}|$ and |$| were allowed to decrease from the upper to the lower end of the line, resulting in slower line speed on the lower end. The direction of $\overline{\mathbb{V}}$ and $ were made to veer from the upper to the lower end in figure 5(c) causing only minor line distortion with time. Figure 5(d), (e), and (f) are further variations on the nearly limitless possibilities for the combinations of $\overline{\mathbb{V}}$ and $, that can act on convective elements and ultimately determine squall-line orientation and motion. Note that the propagation effects increase from the upper to the lower end in figure 5(f), but that propagation plays the dominant role in line displacement at the upper end where the shear component is weakest. It will develop that the situation in figure 5(f) most closely resembles that in the case under study.

It should be pointed out that the $\overline{\mathbb{V}}$ fields displayed in figure 5 are quite similar to those of numerous actual cases examined in connection with other convective outbreaks of the scale under investigation here. That is, changes in mean wind direction, and particularly speed, are small and uniform across the squall-line zone with time. It would seem reasonable that the sudden changes that are frequently observed to occur in squall-line orientation and motion (see figs. 7 and 9) are due mainly to the effects of propagation.

Correlation with upper winds. Most previous investigations of squall-line movement by radar have been limited to lines whose longitudinal extent was less than 200-300 mi. [3,5,7,9]. Those limitations are imposed when only one radar is available for recording the history of a line, because of the range and sensitivity limitations inherent in a single radar. The extensive convective outbreaks that occur in the central United States frequently reach lengths far greater than the range capabilities of a single radar. In the case under study, the squall line at peak intensity was continuous from western Iowa into south-central Texas, a length of 600-700 n. mi.

Following techniques developed by Ligda [15,16], a presentation of the squall line as a whole was prepared at 3-hr. intervals between 1200 and 0000 CST. Film records were available from U. S. Weather Bureau WSR-57 (10 cm.) radars located at Des Moines, Iowa; Kansas City, Mo.; Wichita, Kans.; Oklahoma City, Okla.; and Amarillo and Fort Worth, Tex. The unattenuated (0 db.) scope photography from these radars was traced and projected at a common scale. Individual scope presentations were then superimposed and matched according to appropriate geographic spacing of the stations, orienting the tracing with respect to echo features common to more than one radar. These composite radar displays were then reduced through optical techniques and projected at the scale of the maps on which the mean wind fields appeared. It is this composite radar echo that is shown along with the sea-level isobars in the series in figure 6.

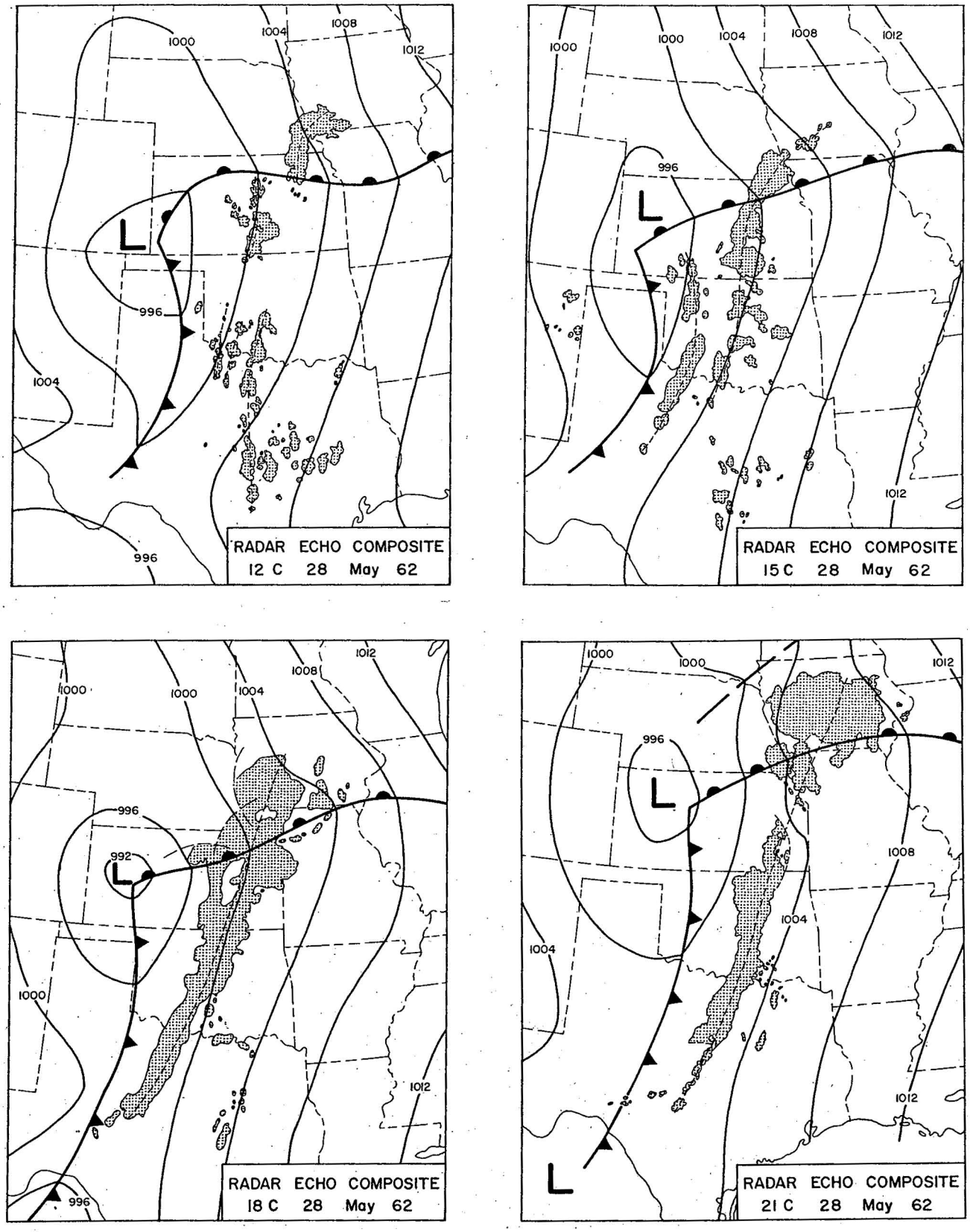

Figure 6.— Sea level isobars and composite radar echoes, May 28, 1962.

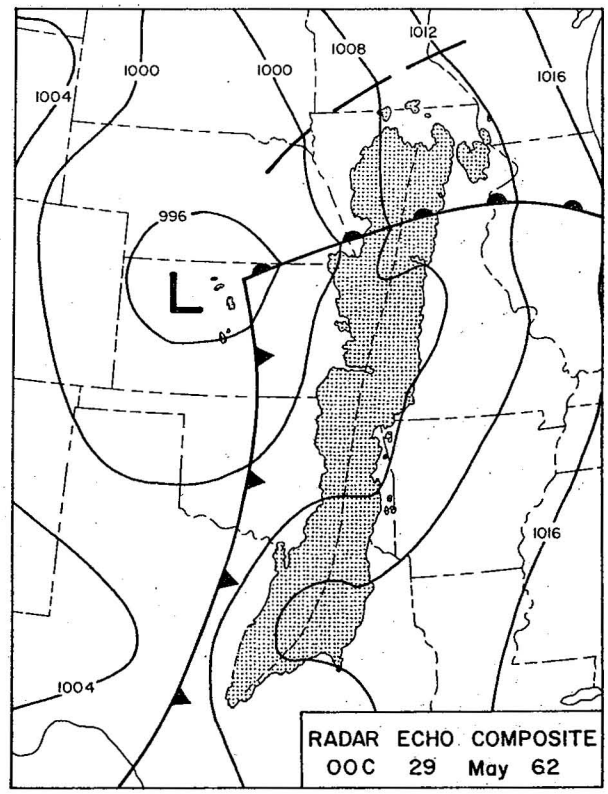

Figure 6.

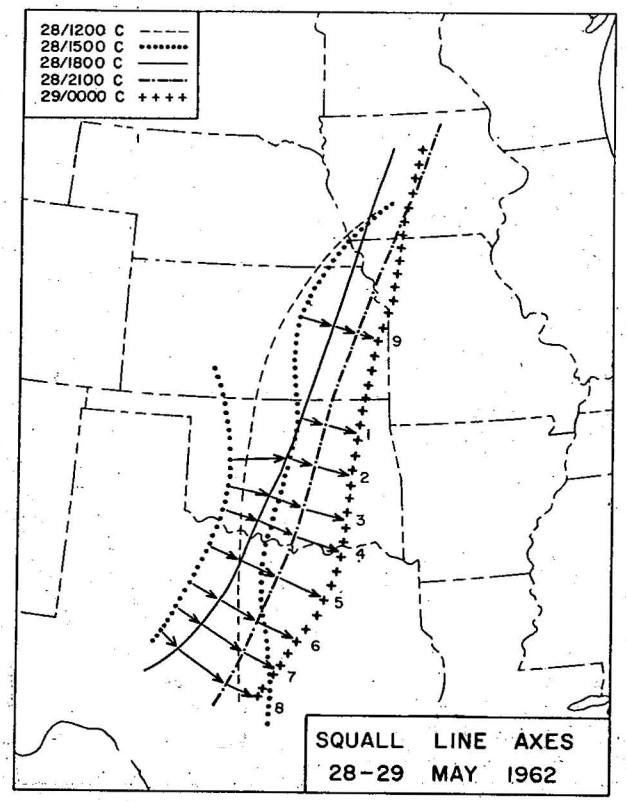

Figure 7.— Displacement of squall-line axes.

The broad width of the squall-line zone as depicted by the unattenuated radar in figure 6 made it difficult to define a unique squall-line axis. Reliable continuity in line displacement could not be obtained for time intervals much shorter than the shortest time interval in wind observations. Furthermore, since complete wind data were not available at intervals of less than 3 hr., line displacement measurements at less than 3-hr. intervals for use in comparison with mean wind were not considered justified. Longer time intervals between measurements of line displacement as well as some smoothing of line features were, therefore, considered necessary in defining line motion at this scale. The dashed lines that appear in figure 6 were taken as the smoothed axis of the squall-line zone and it is the displacement of this axis normal to itself that is correlated with the mean wind fields (see fig. 7).

Correlative wind data were obtained by superimposing the isotach and isogon fields (fig. 4) on the squall-line displacement plot (fig.7) and reading point values of wind speed and direction corresponding to line time and position. The mean wind for a 3-hr. period was considered to be the average of the beginning and ending point values.

Nine speed and direction computations were made across the zone swept out by the squall line as depicted in figure 7 with regard to the line displacement between the hours of 1500 and 0000 CST. The speed of the line was taken as the average speed determined from the total displacement of the line normal to itself. The direction of movement was considered to be the average of the 3-hr. displacement vectors oriented normal to the line.

The computations relating squall-line motion to the mean wind appear in table 1. As evidenced by the data in table 1, both squall-line speed and layer mean wind speed (columns 2 and 3) indicate small and random variation along the zone. The component of mean wind normal to the line contributed on the average 50 to 60 percent of the total line motion. The remaining part of the motion must be accounted for mainly by propagation.

Computation No. 9 is of particular interest in this respect. It will be noted that the mean wind is oriented nearly parallel to the squall-line axis and hence the normal component of mean wind is nearly zero. The results in this area support findings cited earlier [5,7] that for low component wind speeds the formation of new cells ahead of the existing line makes the dominant contribution to line motion.

The most consistent feature in the data presented in table 1 is the angular difference ($\Delta\alpha$) between the mean wind direction and the direction of line displacement. Wind direction shows a gradual veering tendency from the northern end of the zone to the southern end, and there is a corresponding veering in squall-line orientation. This coincident veering of wind and squall-line orientation along the zone results in the high correlation in figure 8. The line motion was on the average 79 degrees to the right of the layer mean wind, and this constant angle $\Lambda\alpha = 79°$ is represented by the 1 : 1 slope in figure 8.

Table 1. Computations Relating Squall Line Displacement to Mean Wind.

Computation	V_L	$\overline{V}$	$\overline{V}_N$	V_N/V_L	$\Delta\alpha(\alpha_L - \alpha_W)$
				(%)	(°)
1	287/13	205/48	287/07	54	82
2	282/17	207/49	282/13	77	75
3	285/18	210/48	285/13	72	75
4	290/18	211/45	290/09	50	79
5	295/18	214/45	295/07	39	81
6	298/18	220/44	298/09	50	78
7	301/17	225/44	301/11	65	76
8	304/16	229/43	304/11	69	75
9	290/10	198/47	290/00	0	92

V_L, squall line movement normal to itself.

$\overline{V}$, mean wind averaged across the displacement interval

$\overline{V}_N$, component of mean wind normal to squall line

V_N, speed of normal component (kt.)

V_L, speed of squall line (kt.)

α_L, direction from which squall line is moving

α_W, direction of mean wind

4. BEHAVIOR OF SQUALL LINE WITH RESPECT TO INDIVIDUAL COMPONENT ELEMENTS

Complex structure within broad-scale squall-line zone. A common feature observed in broad-scale convective outbreaks is the tendency for multiple line structure to exist at a given time within a preferred squall-line zone [3,5,7]. Figure 9 depicts, at 30-min. intervals, the positions of the axes of highest intensity radar echoes that lay within the squall-line zone of May 28, 1962, as it moved across central Oklahoma. Although it was not always apparent on the unattenuated radar return, multiple line structure existed at nearly all times. The average separation between lines was about 20 n. mi. Common orientation and continuity features seldom had a history of

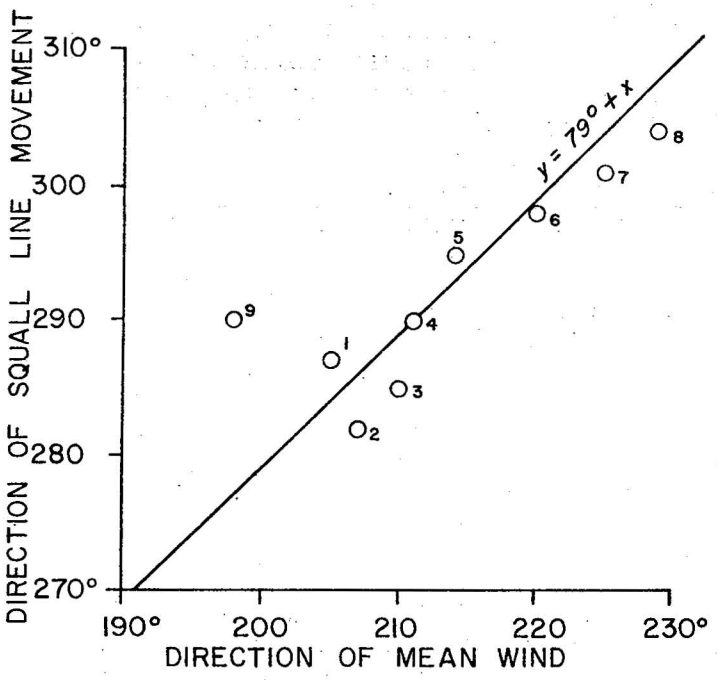

Figure 8.— Correlation diagram; mean wind direction vs. direction of squall-line movement.

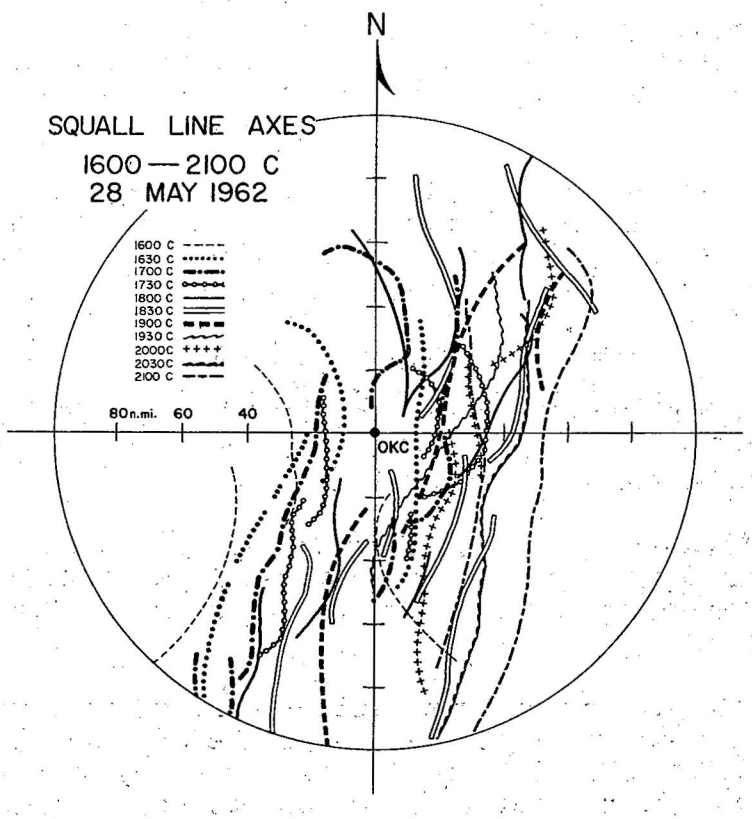

Figure 9.— Squall-line axes at 30-min. intervals within 100 n. mi. of Oklahoma City radar.

more than 2 hr. Apparently as a result of propagation, new lines appeared and intensified and old lines dissipated. Recurrent passage of successive lines over a particular point was frequent. There was a point 35 n. mi. northeast of the radar that was common to 1700, 1730, 1800 and 1900 CST line positions.

Detailed analysis of squall-line segment. In an attempt to separate the component contributions of the translation of individual cells within the axis of a line from that portion of line motion caused by propagation, a detailed sequence plot was made of the life history of a particular line segment in the vicinity of the Oklahoma City WSR-57 radar. (See fig. 10).

From step-gain photography, seven levels of attenuation were available. Three of these levels (12, 33 and 39 db.) were superimposed on each time plot yielding an intensity contour effect. The 12-db. level served to delineate the line structure, and the 33- and 39-db. levels defined the individual high intensity echoes (hard cores).

The line segment had a life history extending over about 5-hr. It formed from large isolated and widely separated (40 to 60 n. mi. apart) echoes at 1330 CST into a solid line structure, at the 12-db. level, by 1500 CST. The time sequence presented in figure 10 covers that period when the line was nearest the radar and at highest intensity. After 1730 CST, the line began to decrease in intensity and length and lost all semblance of line structure by about 1830 CST. During its formative stages, and at maximum intensity, new echoes formed periodically toward the southern end of the line. When this tendency for new echo development ceased, the line began to diminish rapidly.

During the period 1545-1800 CST, 16 individual echoes were trackable with continuity that endured for at least 15 minutes. All of these cells developed near or within the line and eventually formed a part of the line. Their average lifetime as identifiable individuals was approximately 40 minutes with a range of 20 to 86 minutes. The most frequent life span was from 30 to 40 minutes. Considering the longevity of these echoes and accepting evidence in this respect presented by previous investigators [4,7,8,21], it seems likely that we have approached the resolution where new convective element growth and old element decay are discernible.

Even though these segment cores lay within a relatively small area with respect to the uniform broad-scale wind pattern, appreciable differential movement is portrayed by their tracks that appear in figure 11.

Speed and direction computations were carried out on the echoes, and their motion was then correlated to the mean wind. A frequency distribution (fig. 12) of echo direction displays a very nearly symmetrical distribution about the 850-300 mb. mean wind. There are two

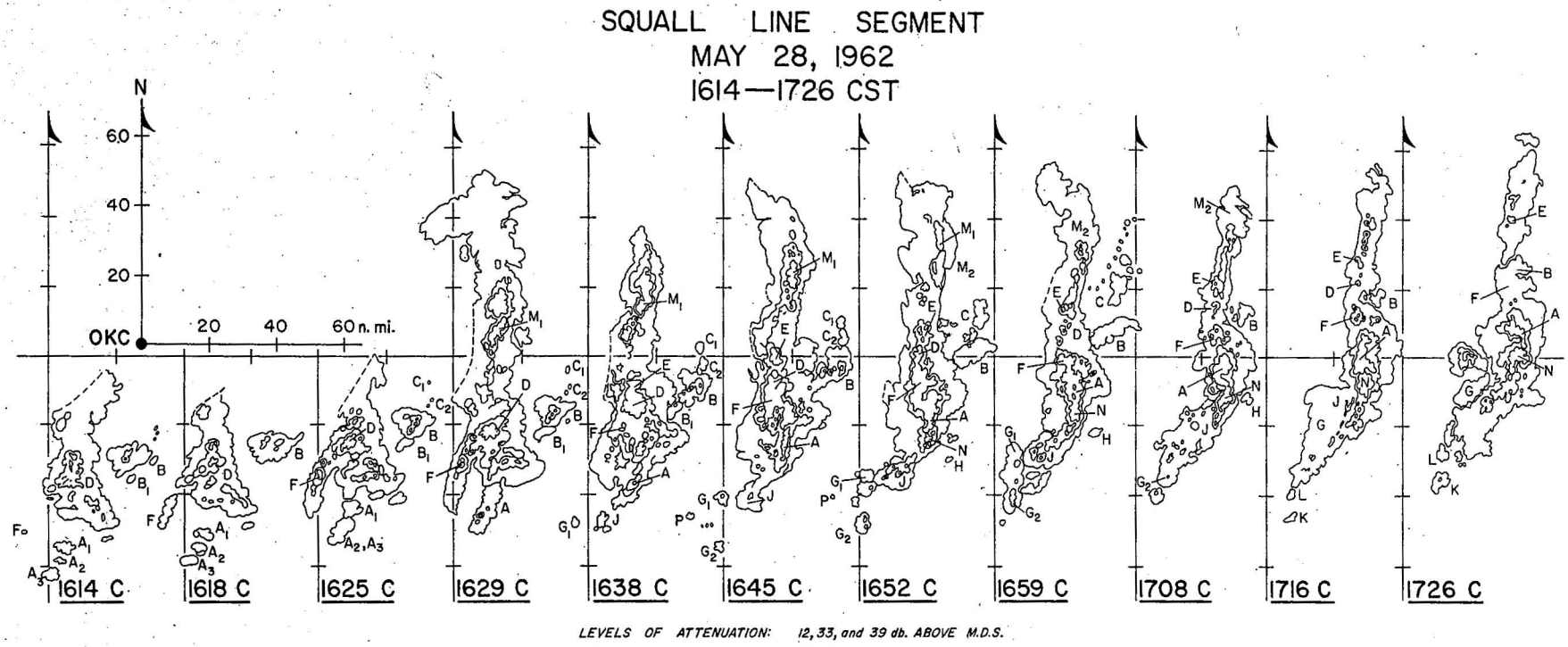

Figure 10.— Sequence display of a segment of the main squall line in the vicinity of Oklahoma City radar.

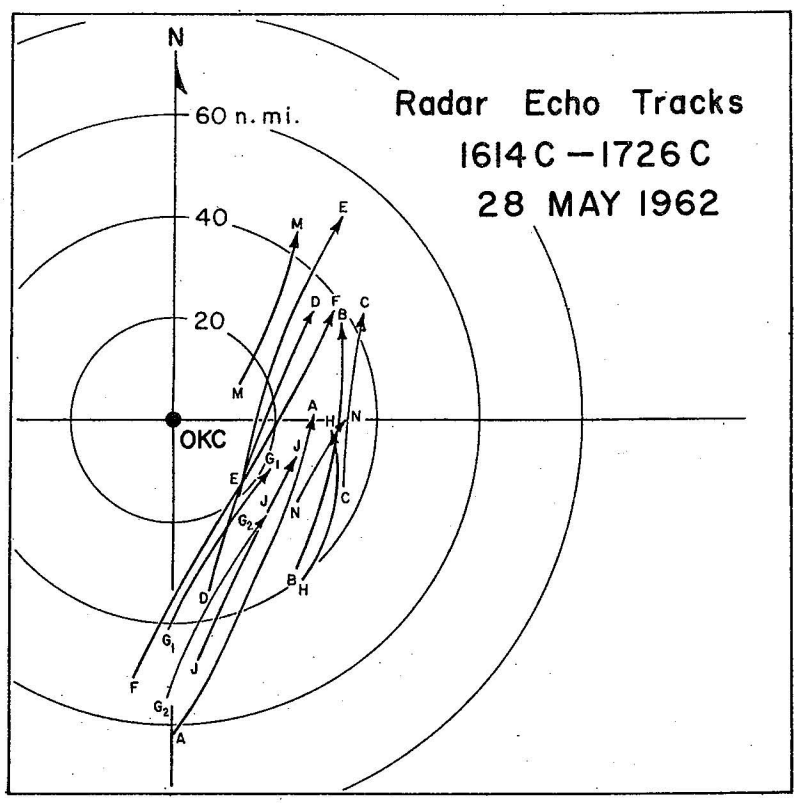

Figure 11.— Individual tracks of echoes comprising squall-line segment displayed in figure 10.

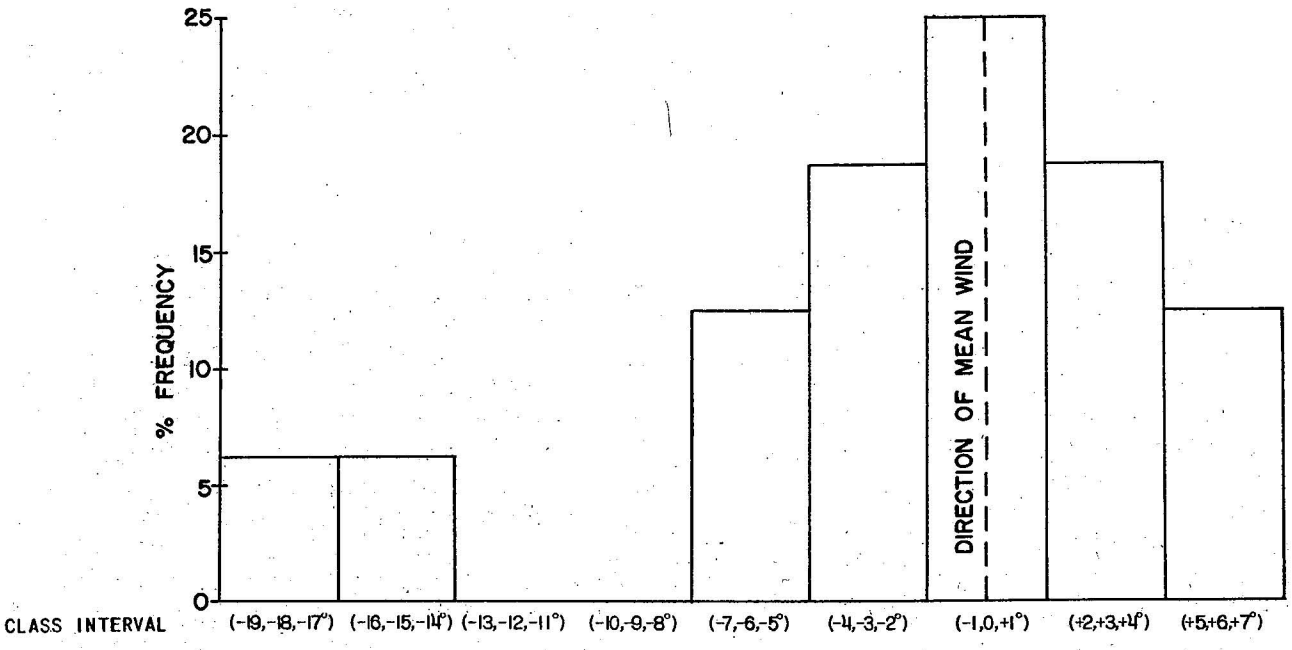

Figure 12.— Frequency distribution of angular deviation of the direction of movement of echoes within squall-line segment from mean wind direction.

notable exceptions. The class intervals lying far to the left of the mean wind contain one occurrence each. These are echoes C and H in figure 10. Neither echo reached the 33-db. intensity level, and it is proposed that the broad-scale steering flow affecting these weaker echoes was restricted to the lower levels which at this time had directions that are to the left of the mean wind for the total 850-300 mb. layer. Also, the exaggerated and localized effects of low-level confluence probably played some role in deflecting these smaller cells to the left, since their positions with respect to the main line segment are in an area where the effects of low-level confluence could be expected to be at a maximum (fig. 3a).

Comparisons of echo speed with mean wind speed revealed that the "cores" moved consistently faster than the environment as defined by the mean wind. The average mean wind speed in the vicinity of the line segment was 46 kt., or about 75% of the average echo motion of 61 kt. (fig. 13). Explanation for this deficiency in mean wind speed compared to total echo motion is difficult, but at least one source can be identified. Detailed examination of the vertical profile of proximity wind soundings revealed that a broad zone of strong flow existed in lower layers. The excessive smoothing in the mean wind computation technique (discussed in Section 2) appears to have reduced the estimate of the total effective flow through the layer.

In the case of most of the individual echoes that eventually comprised the line, it was possible to determine their direction and separation from the nearest existing hard-core echo at the time of initial appearance. New cells showed a predominant tendency to form on the upwind (SW) side of the line segment (fig. 14). However, there was a great deal of variation in their locales of formation with respect to existing elements. Echoes C_1 and C_2 (see fig. 10) developed to the northeast of the large echo B, and H first appeared southeast of the nearest line segment. Echo E made its first appearance as a separation from the northern part of D and is an example of new growth on the leading edge of an existing cell. Echo N also appeared as a separation from an existing element when it began to break away from the southern portion of A.

For those cases where new echoes first appeared separated from the line, their duration as unattached individuals ranged from 6 to 105 minutes. Echo F began as a point (first frame of figure 10) and blossomed into a 39-db. line component in 10 minutes, while B reached maximum intensity and remained a separate entity ahead of the main line for over an hour before diminishing and turning into the forward portion of the line. Series A and G both added length to the southern end of the line; however, G lagged behind the main line structure, whereas A moved into and became a major component of the main line. The A series looks rather insignificant at 1614 CST, but it eventually produced a tornado on the ground near Shawnee, Okla. at approximately 1720 CST. L and K (last two frames of fig. 10) took a position even farther to the rear of the line, and later film history indicates that

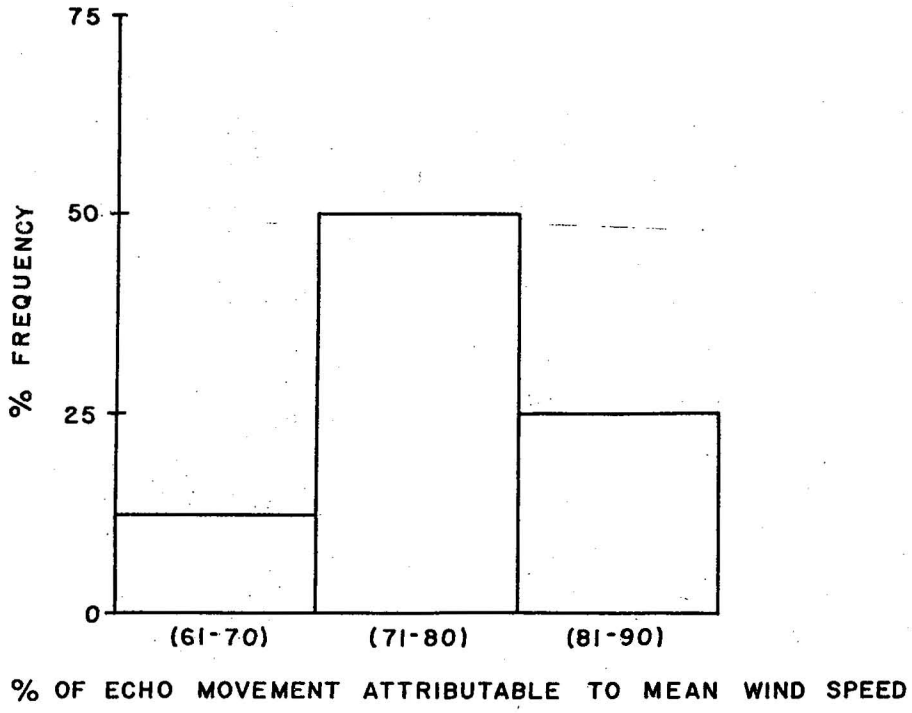

Figure 13.– Frequency distribution of the percent of echo motion attributable to mean wind speed for echoes within squall-line segment.

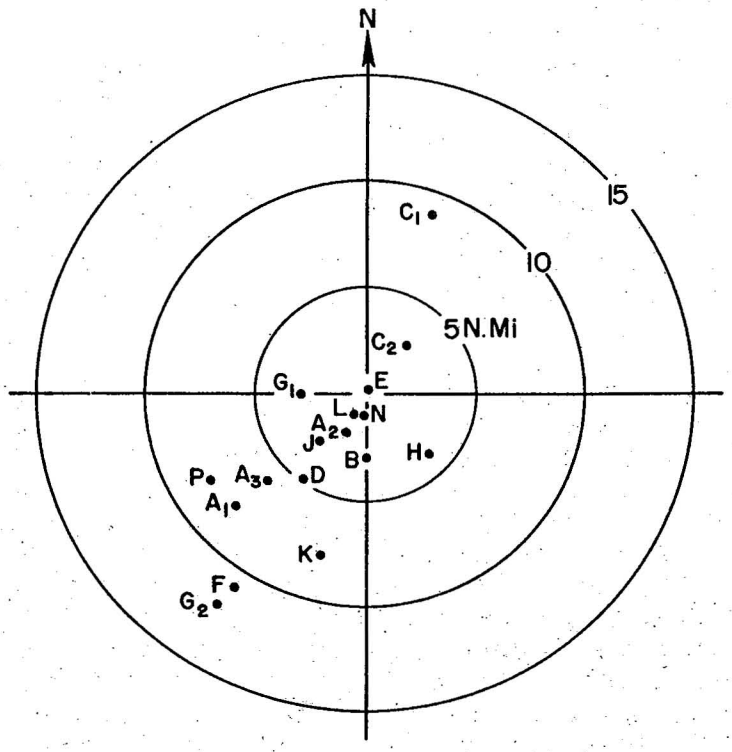

Figure 14.– Position of echo at the time of initial appearance with respect to nearest existing line element (represented by the center of the range circles).

they contributed to the formation of a second line, typifying the process whereby multiple line structure evolves.

Summary. The foregoing discussion in Sections 3 and 4 is intended to point out the complexities involved in attempting to define line motion at various scales. It is appropriate at this point to summarize some of the relationships between the movement of individual storms and the squall line as a whole that revealed themselves in the detailed analysis described in this case. Examination of other cases revealed the same general characteristics [20].

(a) New elements tended to form on the upwind (SW) side of an existing line segment.

(b) The elements, moving faster than the line as a whole, passed through the line segment and eventually dissipated on the downwind (NE) side.

(c) New growth was added to the line by two different processes:

1. The accretion of new elements, which were at earlier times isolated echoes, usually located ahead of or on the southwest end of the line, and

2. The growth of new cells within and immediately adjacent to the southwestern end of the existing line.

(d) When new cell growth ceased, line segment length and intensity diminished rapidly.

(e) Storms ahead of the line tended to move toward the left in comparison with those within or on the southwestern end of the line, thereby being eventually overtaken by the line.

(f) Isolated storms which formed earliest had the longest lifetimes, suggesting that cells within the line grow and survive at the expense of their neighbors, while isolated storms feed freely off the environment.

5. INDIVIDUAL STORM STUDIES

A basic requirement for investigating the motion of individual convective storms through the use of radar is high-quality, detailed scope photography. The Weather Bureau's WSR-57 radar, located at Will Rogers Field, Oklahoma City, Okla. recorded what can be considered to be excellent radar scope photography concurrent with the squall-line situation of May 28, 1962. Scope photography was available for the entire 24-hr. period of the 28th and extended continuously into the morning hours of the 29th. A step-gain attenuation program was

being run beginning at approximately 1245 CST on the 28th and continuing into the 29th. Scanning range was 250 n.mi. until 1400 CST, and another period of 250 n. mi. scanning was run between 1820 and 1920 CST. During the remainder of the day the radar was set to scan the 100 n. mi. range.

Between the hours of 1200 CST and 2100 CST, 35 individual thunderstorm complexes were studied in great detail. Persistent line development did not occur until about 1500 CST, and prior to this time isolated echoes were the predominant feature under investigation.

Definition and analysis. A complete tracing of the enlarged radar film scope presentation was made at intervals of 15 min. or less, using a tissue azimuth-range overlay. Of the seven levels of attenuation (0,12,21,27,33,39 and 45 db. above MDS) built into the step-gain program, six were traced at each time interval, using a color scheme for the identification of particular decibel levels. The 27-db. level was eliminated because it was found that only slight image reduction took place between the 27-db. and 33-db. steps. An example of the typical step-gain sequence is presented in figure 15.

It has already been pointed out in Section 3 that greater signal return from high intensity storms during periods of vigorous convective activity tends to agglomerate echoes within a line. For this reason, levels of low attenuation saturated the scope with echo return and failed to yield sufficient detail for identifying any of the small-scale features within the squall line. During a particular attenuation program, the step that first began to yield separation in echo structure was usually the 21-db. level. The complexes outlined at the 21-db. level were also those that most frequently provided continuity from one time interval to the next. Higher levels of attenuation served to depict the so-called "hard core" of the individual echo complexes. The "hard core" was accepted as a measure of intensity, but it was usually the 21-db. echo image that then was used for echo movement calculation. Computations were made, however, only for those storm complexes that generated at least a 33-db. hard core at some time during their lives.[2]

Those echo complexes that appeared to possess continuity in shape, size and displacement from one 15-min. interval to the next were plotted on a single tracing overlay. The echo centroid was estimated by ascribing a "best-fit" geometric simplification (i.e., rectangle, circle, or ellipse) to the echo contours. The speed ascribed to the complex was the average speed resulting from the total displacement during its identifiable life history. The direction of echo movement was taken as the single vector having a best fit with respect to each 15-min. displacement vector.

An evaluation of the comparative accuracies involved in the speed versus direction calculations will reveal that far greater confidence

---

[2] 33 db. corresponds approximately to a reflectivity of $z = 2 \times 10^3 \text{ mm}^6/\text{m}^3$ at 50 n. mi. range.

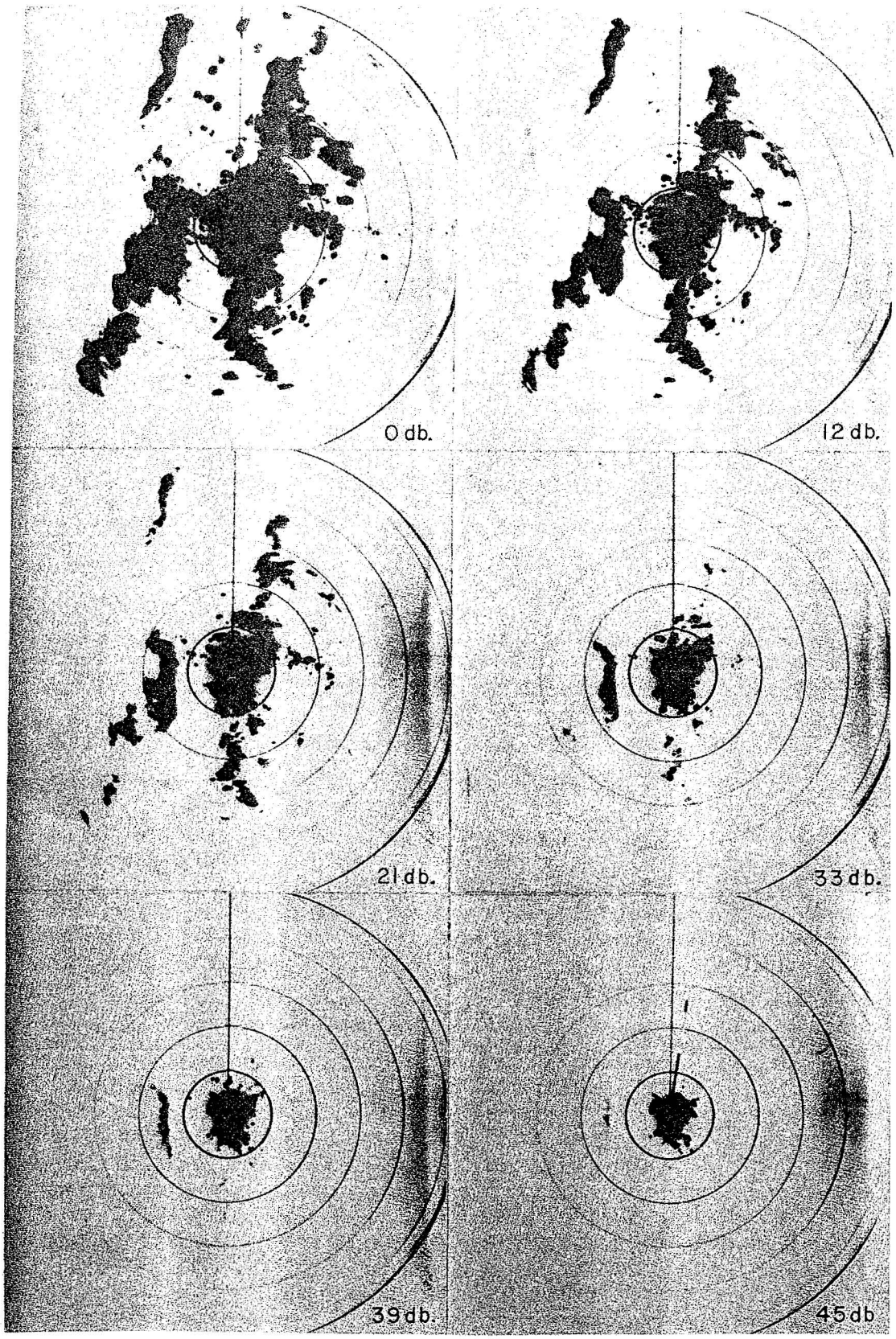

Figure 15.— Typical radar film display of a step-gain program, May 28, 1962, 1600 CST. Levels of attenuation left to right from top (0, 12, 21, 33, 39, and 45 db. above MDS). Range markers 20 n. mi. intervals.

can be placed on the direction of movement. Attempts to determine echo motion from radar scope photography are complicated by inherent limitations in the interpretations of the film presentation. Among these limitations are: (1) difficulties in separating the translation of individual cells within a complex from that portion of motion caused by propagation; and (2) the effects of range attenuation. Over longer time intervals, the evaluation of speed is more seriously affected by these factors than is the evaluation of direction.

Persistence of storms. Although significant variations existed in the motions of different storms (fig.16), each individual complex possessed a high degree of persistence in speed and especially direction.

The average lifetime of the 35 echo complexes on which movement computations were made was 80 min. The period of existence as identifiable individuals ranged from 40 to 195 min., and the most recurrent lifetime was from 60 to 75 min. The period of observation was occasionally restricted by the radar range and the loss of continuity caused when an echo moved into the "ground clutter." In seven of the 35 cases, the echo history was interrupted by the range limits of the radar, and eight times continuity was lost by ground clutter masking. Both range and ground clutter affected the observed history of three complexes. For 23 cases, where continuity was uninterrupted by either range or ground clutter, the average lifetime was 70 min.

The diameters of these systems varied from 5 to 25 n. mi. at the 21-db. level of attenuation, and the average diameter was around 10 n. mi. Although size of an echo at a particular decibel level is range dependent, no effort was made to account for this range attenuation in evaluating the diameters of the echo complexes.

Referring again to evidence presented by previous investigators concerning lifetime and size of individual cells [4,7,8,21] we may conclude that the element that is tracked in this study is not an individual thunderstorm cell but rather a generating system. These generating systems may be composed of one or more individual cells at a particular time. Since the complexes survive for periods of an hour or more while the cells that compose them decay and regenerate, we have, as in the case of the main large-scale squall line, the component contributions of translation and propagation.

Storm motion vs. mean wind correlation. Procedures followed in the computation and analysis of the layer mean wind have been discussed in Section 2, and the evaluation of echo motion is described in the preceding paragraphs. For purposes of correlating mean wind with echo motion, the mean wind isotach and isogon field were superimposed on the echo displacement plots. Point values of wind speed and direction were read at positions corresponding to the mid-point of the echo path. Since wind fields were available only at intervals of 3 hr., some interpolation in arriving at wind values was necessary. If the mid-point of an echo history was within an hour of a particular wind analysis, wind data for that time were accepted. When the center of an echo history was separated by more than an hour from a wind analysis the point values from the two nearest map times were averaged. These procedures may be considered to be justified since the wind patterns were changing very

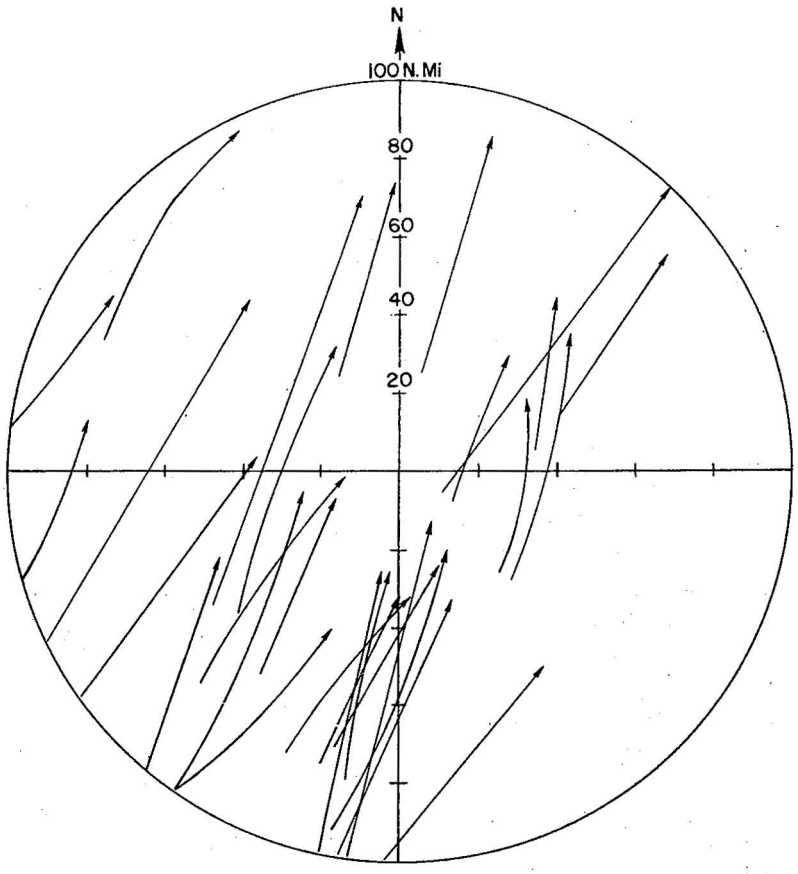

Figure 16.— Individual storm tracks during afternoon and evening of May 28, 1962, within 100 n. mi. of Oklahoma City radar.

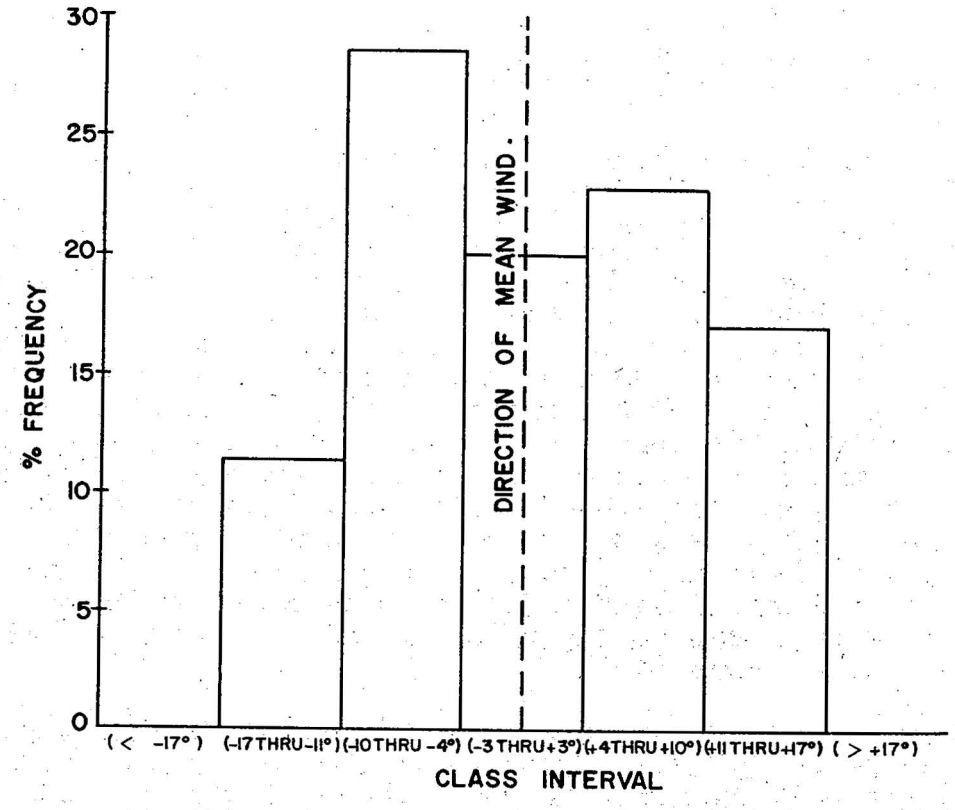

gure 17.— Frequency distribution of the angular deviation of storm path from mean wind direction.

slowly (see fig. 4).

Figure 17 shows the frequency by 7° class intervals of the angular difference between the direction of mean wind and the direction of echo movement. Over 70% of the echoes moved from a direction that was within 10° of the mean wind and all echoes moved within 15°. A nearly symmetrical concentration around the mean wind direction is suggested. The standard deviation of the sample with respect to the mean wind was 9°.

As in the case of the hard cores within the squall-line segment (Section 4), there was a significant percentage of echo complexes that moved faster than the environment flow as defined by the layer mean wind (see fig. 18). Here again, part of the excess motion can be explained as the result of excessive smoothing in the mean wind computation technique. A second possible explanation lies in the change of wind with height and the fact that the echo complexes under study were very likely propagating.

It has been proposed [19] that growth of new convection is most favored on the downshear side of an existing storm. If this proposition is accepted, the favored area for growth would be on the forward portion of an existing cloud if the wind increases with height and there is little directional shear. Figures 1 and 2 indicate only small veering of wind with height over the convective storm area. It is then conceivable that a portion of echo motion in excess of the mean wind can be attributed to propagation in this case. Unfortunately, because of the limited resolution of detail by the radar, the effects of new growth on the movement of individual echo complexes could not be substantiated in all cases and the above statement must remain qualitative.

Variability and scatter in storm behavior. In the case of the "hard cores" within the squall-line segment (Section 4), as in the study of propagating echo complexes described in this section, there was a great deal of scatter in echo behavior within a nearly uniform wind field. It is clear that these variations are real and not entirely due to uncertainties in wind and echo movement computations. Variations in individual storm behavior are believed to be due to randomness in new cell formation. Some of the scatter can be understood and taken into account in terms of the character of the wind field and the comparative sizes of the convective storms. Newton and Katz [18] suggested that the role of the environmental wind field is not merely one of transporting existing thunderstorms, but that its character may also govern the structure and behavior of the storms themselves. It was concluded in a study of five synoptic cases in which there was appreciable veering of wind with height that, as an average condition, larger storms tended to deviate more to the right of the mean wind and move more slowly than smaller storms [20].

It was impossible to determine any systematic differential motion in this storm sample with regard to size or intensity of an echo complex and its deviation from the mean wind direction. This is probably

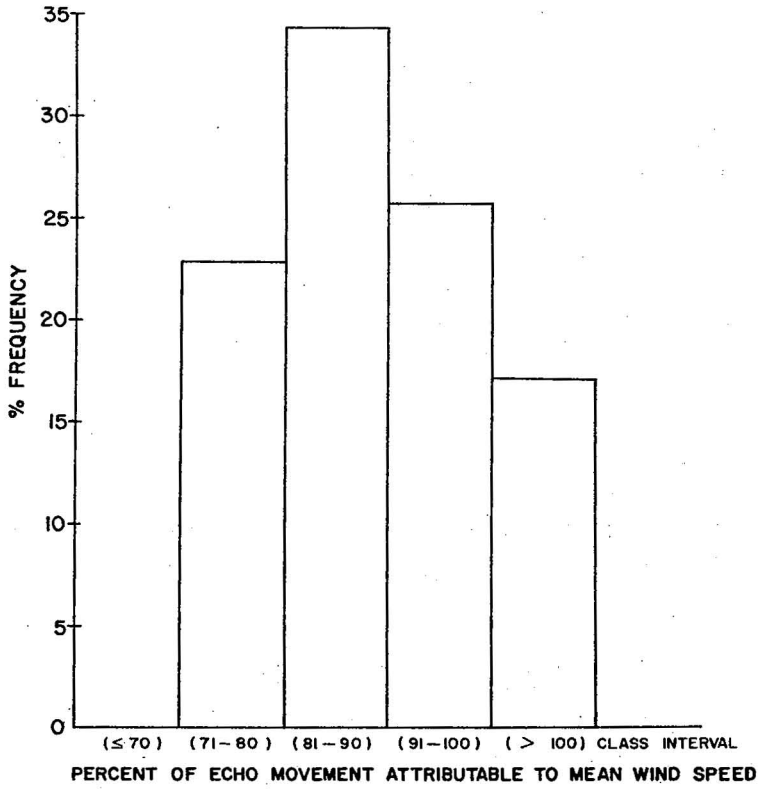

Figure 18.– Frequency distribution of the percent of storm speed attributable to mean wind speed.

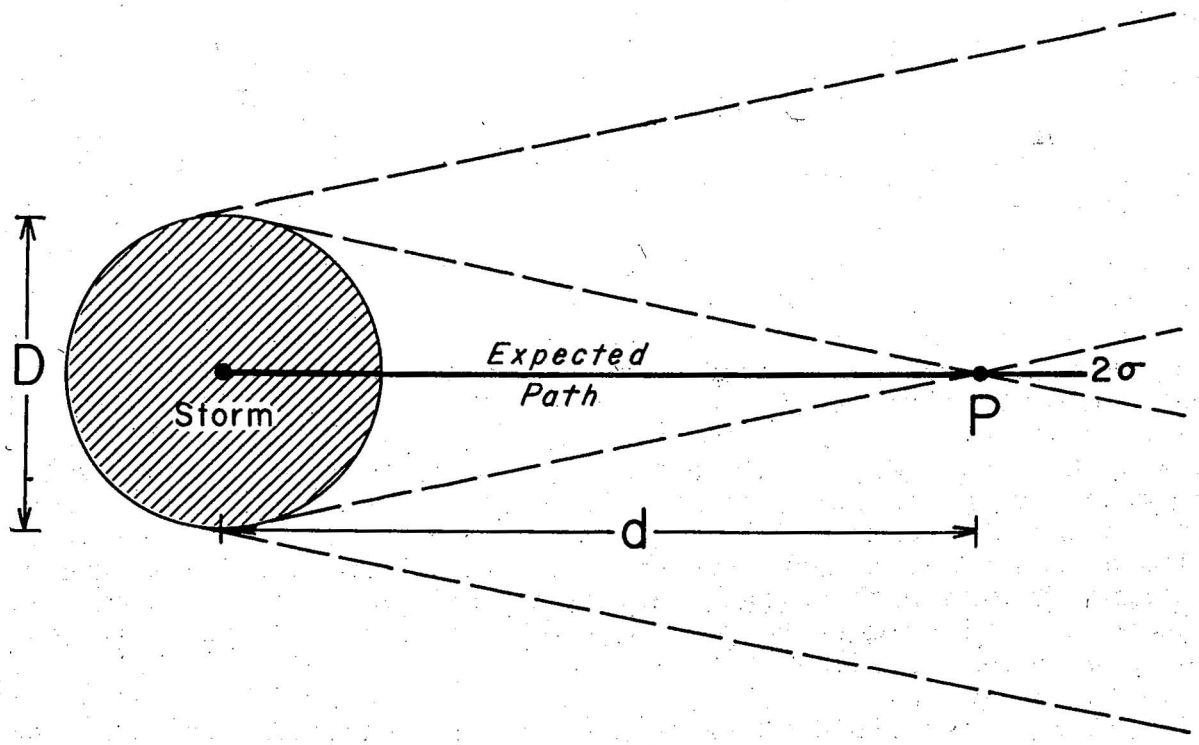

Figure 19.– Depiction of probability of movement of a storm of diameter D over a point P at a distance d downwind from the storm, where σ is the standard deviation from the most probable direction. (See text.)

due to the fact that storm size was nearly uniform and that the range of wind directions was relatively small.

A large degree of variation in storm behavior cannot be explained in terms of the upper winds alone and must be attributed to our failure or inability to consider and define the contributions of other parameters such as potential instability, orographic effects, etc. It is essential, however, to establish some measure of the degree of variation in storm movement versus mean wind because this sets a limit on success which can be achieved in forecasting storm motions.

6. ON THE PREDICTABILITY OF CONVECTIVE STORMS

The ultimate objective in investigating the movement of radar-detected storms is to predict the time and likelihood of their passage over a point on or near their projected paths. Once the statistical scatter of a storm sample around the mean wind for a given upper-wind situation has been established, the problem of the vulnerability of a point may be approached through the application of the theory of probabilities.

For the purposes of qualitative discussion refer to figure 19. This schematic diagram illustrates the case in which a storm of diameter D lies directly upwind from a point of interest, P, (e.g., an airfield or a point on an airway). With a normal distribution of the scatter of storm movements around the mean wind direction, 68 percent of the possible storm paths will be confined within a range of $\pm\sigma$. Thus about two-thirds of the time, the storm paths will be within the angular limits shown by the dashed lines. Points lying a distance d downwind along the most probable direction of storm movement possess a two-thirds or greater expectancy that some part of the storm will pass over them. Points farther downwind possess a less than two-thirds expectancy that the storm will pass over them. The degree of success in forecasting storm passage depends on the use made of these probabilities.

From the diagram in figure 19, the angle $2\sigma = D/d$, or $d = D/2\sigma$ (radians), and since 1 radian $\approx 57°$,

$$d \approx \frac{28D}{\sigma} \quad \begin{matrix}(\text{storm diameters}) \\ (\text{degrees})\end{matrix}$$

This equation demonstrates the importance of knowing the degree of scatter.

Application of probability theory. Consider the evidence presented in preceding sections that, for the special case of small turning of wind with height, thunderstorms tended to move along the direction of the vector mean wind in the cloud-bearing layer. In addition, assume the frequency distribution of the deviations in storm direction from the vector mean wind to be normally distributed (see fig. 17). Recall also that the standard deviation (σ) of the sample was 9°, and that the average diameter (D) of the echo complexes was 10 n. mi.

With these conditions in mind, the first step in the application of probability theory was to divide the area under the probability curve for a normal distribution, lying between 2 σ to the right and left of the mode, into 1° class intervals (36 classes in this case). (See fig. 20). Any of the 18 radials (± σ) originating at the center of an echo upstream are considered to be possible storm paths, 68 percent or approximately two-thirds of the time. The 18 radials beyond ± σ are then possible storm paths less than one-third of the time.

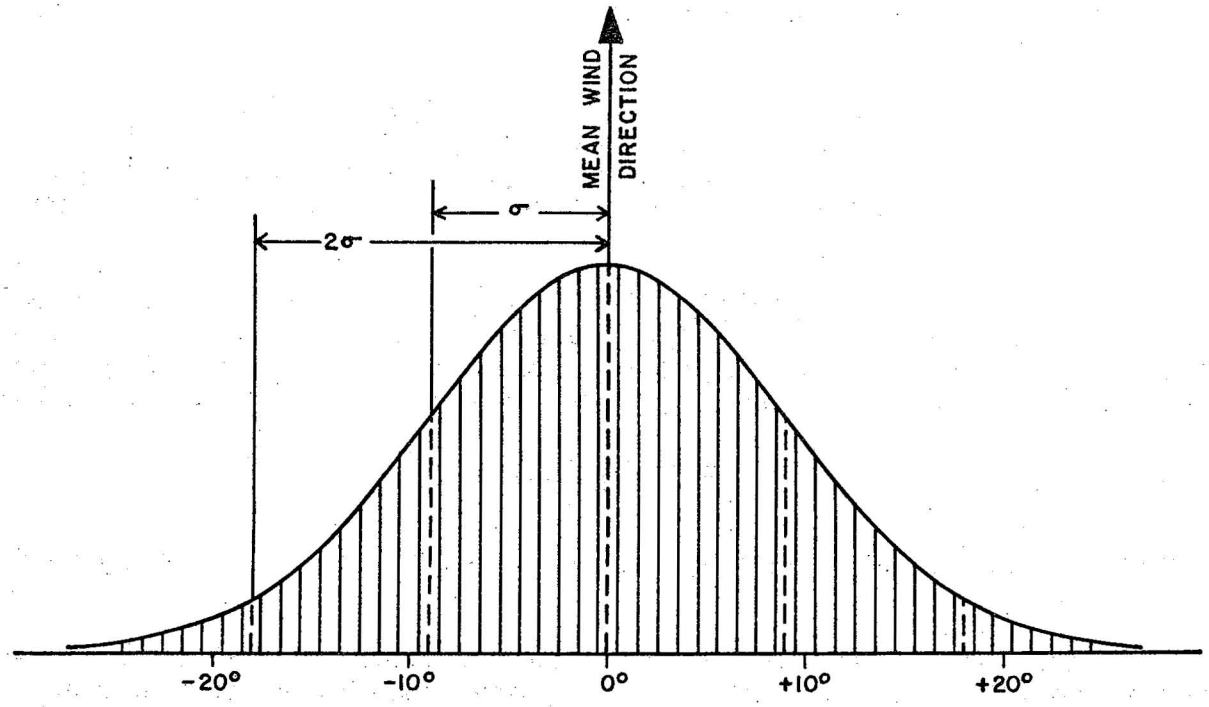

Figure 20.– Probability curve for normal distribution, with area divided into 1° class intervals, where standard deviation, $\sigma = 9^{\circ}$.

Since a radar echo is not a point, the angular width of an echo at a particular range had to be considered. At 20 n. mi. range an average-sized echo with **D** = 10 n. mi. would have an angular width of $\frac{1}{2}$ radian or 28.6°. For the situation where point-echo separation was 20 n. mi. the probability that some part of the storm echo would pass over a point 20 n. mi. downstream along a given radial originating at the echo was taken to be the sum of the areas represented by the individual class intervals which lay 14° ($\frac{1}{2}$ angular echo width at 20 n. mi. range) either side of the radial in question. This procedure was followed for each of the 36 possible storm path radials between ± σ (See fig. 20). Since the angular width of the echo with **D** = 10 decreased with increasing range, the probabilities for each radial also decreased with range. For a storm 50 n. mi. upstream, the angular width of the echo was 11.5° and the probabilities of the individual 1° classes were summed over intervals of 5.75° either side of the appropriate radial. Angular width decreased to 5.75° for echoes 100 n. mi. upstream so that the summation was made across intervals of 2.87°.

The application of the foregoing arguments yielded the probability curves for point-echo separations of 20, 50 and 100 n. mi. which appear in figure 21. The evaluation of station vulnerability from figure 21 may be approached from two standpoints. First consider an echo upstream on a particular mean wind streamline; now, a point lying 50 n.mi. downstream but 5° to the left or right of the streamline passing over the echo has a 45% probability of being affected by the storm. As a second condition let a point 20 n. mi. downstream from an existing storm have a particular mean wind direction, and let the echo motion be 5° to the right of the wind; then the vulnerability of the point is 84%.

It is obvious that the probability of a point being affected by a particular storm, whose projected path brings it near that point, decreases rapidly with increasing range separation between point and storm. Vulnerability has also been shown to be highly dependent on storm size [20].

Forecasting storm arrival. Once the point vulnerability has been assessed, the elapsed time before the storm arrives is of utmost importance. The time in minutes (Δt) required for a nonaccelerating echo complex to arrive over a point in its projected path is expressed by:

$$\Delta t = d/V_E \times 60$$

where d is the range separation (n. mi.) and V_E is the echo speed in kt.

In order to relate elapsed time before storm arrival (Δt) to mean wind speed ($\bar{V}$), it was necessary to employ the correlation between echo speed (V_E) and mean wind speed ($\bar{V}$). The relationship between V_E and $\bar{V}$ is determined by some proportionality factor (k), which is dependent on the character of a unique wind field, such that $V_E = k\bar{V}$. If the standard deviation of the echo speed (σ_{V_E}) about the mean wind speed for a given wind situation is taken into account, the elapsed time before storm arrival can be written:

$$\Delta t = d\left(\frac{1}{k\bar{V} \pm \sigma_{V_E}}\right) 60$$

In the discussion of echo versus mean wind speed in Section 7, it was pointed out that echo motion exceeded the mean wind speed in the majority of cases. (See fig. 18). The average contribution of mean wind speed toward echo motion was 89%, so that for this case:

$$\bar{V}_E = k\bar{V} \cong 1.12\bar{V}$$

The standard deviation (σ_{V_E}) of echo speed from mean wind speed was 9 kt.

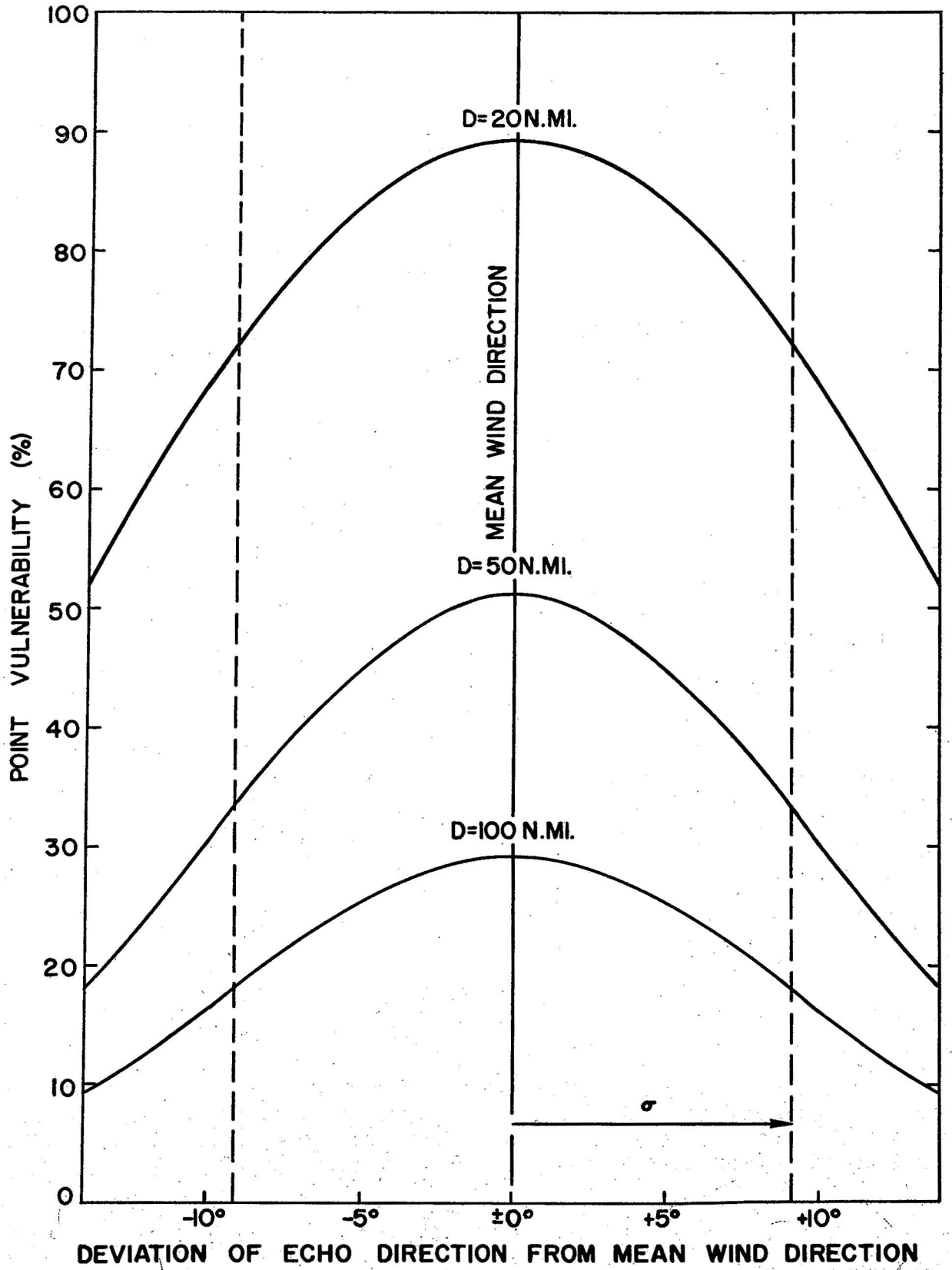

Figure 21.— Point vulnerability nomogram. (See text.)

Curves for a point-echo separation of 10 n. mi. resulting from the plot of $V_E = k\bar{V} \pm \sigma_{V_E} = 1.12\bar{V} \pm 9$ are shown in figure 22. To determine the forecast time increment before storm arrival when point-echo separations are multiples of 10, it is necessary only to increase the time resultant for 10 n. mi. range separation by the appropriate multiple.

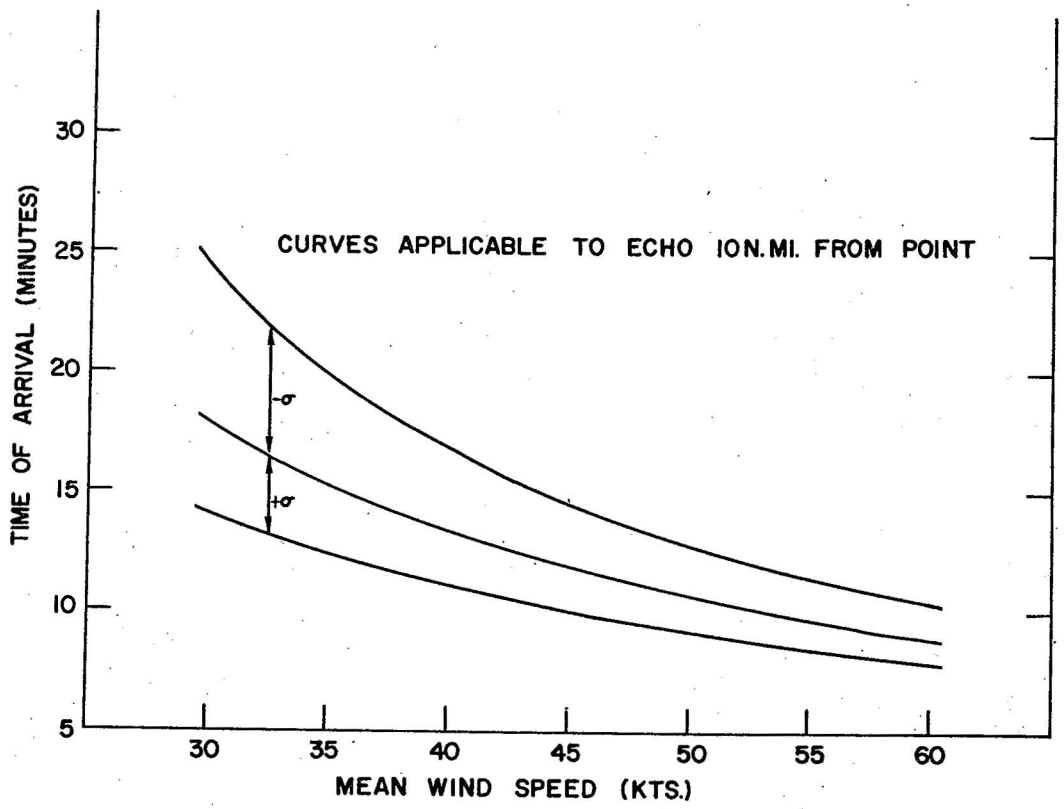

Figure 22.— Time of arrival of an echo over a point in the projected echo path as a function of echo-point separation and mean wind speed. (See text.)

It is clear from figure 22 that as echo speed (a function of mean wind speed) increases, the accuracy in forecasting storm arrival time increases. Unfortunately, available evidence [20] indicates that large storms show a tendency to move more slowly, so that when time of arrival becomes most critical, the error in forecasting becomes greater.

7. SUMMARY AND CONCLUSIONS

Squall-line motion and orientation are dependent on the rate of development and motions of the individual convective elements which comprise the line. Element motion consists of the two components - translation and propagation. It has been proposed that the translation of convective complexes is related in a systematic way to the mean wind through the tropospheric layer in which the clouds are embedded, and that this relationship is dependent on the unique character of the wind

field. That portion of motion contributed by new growth or propagation will, in a later paper, be shown to be theoretically related to the degree of vertical shear.

In the case of May 28, 1962, in which there was small turning of wind with height, the deviations of storm motion from mean wind direction were small and nearly normally distributed around the mean wind. Propagation effects on storm movement were manifested as storm motions in excess of the environment flow.

Observations of scatter in storm movement around the mean wind direction and the variability of individual echo paths within a nearly uniform wind field are largely real and not due entirely to uncertainties in computation and analysis techniques. This scatter and variability is thought to be due mainly to randomness in new cell growth. Some of the anomalous motion of large storms can be explained in terms of the character of the upper winds, but a great deal of the random motion cannot be explained in terms of the winds alone and must be due to other parameters which are neglected, difficult to define, or not observed.

Once the degree of variability of a storm sample for a given unique upper-wind situation has been established, the problem of predictability can be approached on a probability basis. The vulnerability of a point lying in the projected path of an existing storm is highly dependent on storm-point separation and on the size of the storm. Accuracy in forecasting storm arrival increases with storm speed, which is considered to be a function of mean wind speed.

Discussion and treatment of the convective storm motion problem in this report apply to the relationship between storm behavior and layer mean wind for the case in which there is only slight veering of wind with height. Changes in the character of the wind field from one convective situation to the next, more than likely, produce unique relationships between storm motions and the mean wind field. In seeking the answers to the thunderstorm-steering-flow problem through the correlation of radar echo motion with mean wind, it is necessary to use a combined physical and statistical approach. Each situation must be considered on its own merits, and a great number of cases with varying degrees of wind shear and veering with height must be studied before the whole range of storm behavior can be adequately described in terms of the upper winds.

The amount of time and labor involved in the type of analysis presented in this report is considerable. Current advances in the application of automatic data processing to weather radar studies, along the lines suggested by Kessler and Russo [12] and the developers of STRADAP [2], will facilitate the digestion of far greater quantities of the enormous amount of available radar data. The development of these modern computer techniques should rapidly and efficiently provide to both the researcher and forecaster a volume of information concerning the gross statistical properties of weather radar echoes. It will

remain, however, for the forecaster concerned with the prediction of the motion of a particular thunderstorm or convective complex, to consider the physical implications of the unique synoptic situation which confronts him.

ACKNOWLEDGMENTS

The research reported in this paper to large extent was carried out while the author was with the National Severe Storms Project, Kansas City, Mo. (Director, Mr. C. F. Van Thullenar). The gathering and analysis of the data were supported in large part by the Federal Aviation Agency. Figures used herein were drawn mostly from the Final Report, "Severe Storm Detection and Circumnavigation," FAA Contract ARDS-A-176, Unit IV-A, prepared by NSSP [20].

Appreciation is expressed for the very helpful criticisms and suggestions made by the staff at NSSP. In particular, the author wishes to express his sincere gratitude to Dr. C. W. Newton (formerly Chief Scientist, NSSP) for his stimulation, guidance, and assistance in the preparation of this report. The collaboration of Mr. L. D. Sanders in developing the techniques for the application of probability theory in Section 6 deserves special acknowledgment. The able draftmanship of Mrs. Catherine Wright and Mr. Doyle Perry contributed much to the drawings.

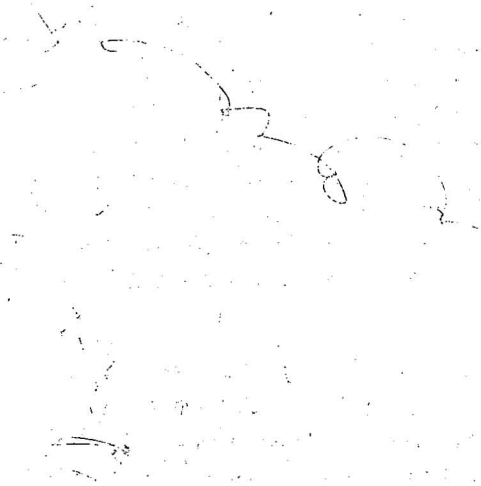

REFERENCES

1. Atlas, D., et al., "Severe Local Storms," Meteorological Monographs, vol. 5, No. 27, American Meteorological Society, Boston, 1963, 247 pp.

2. Atlas, D., H. J. Sweeney, and C. R. Landry, "STRADAP (STorm RAdar DAta Processor) Performance," Proceedings Tenth Weather Radar Conference, American Meteorological Society, Boston, 1963, pp. 377-383.

3. Austin, P. M., "Microstructure of Storms as Described by Quantitative Radar Data," pp. 86-92 in "Physics of Precipitation," Geophysical Monograph No. 5, American Geophysical Union, Washington, D. C., 1960.

4. Battan, L. J., "Some Properties of Convective Clouds," Nubila, vol. 4, No. 1, 1961, pp. 1-2.

5. Boucher, R. J., and R. Wexler, "The Motion and Predictability of Precipitation Lines," Journal of Meteorology, vol. 18, No. 2, April 1961, pp. 160-171.

6. Browning, K. A., "The Basis of a General Model of the Airflow and Precipitation Trajectories Within Persistent Convective Storms," Conference Review for Third Conference on Severe Local Storms, American Meteorological Society, Champaign-Urbana, Ill., October 1963, 16 pp.

7. Byers, H. R., and R. R. Braham, Jr., The Thunderstorm, U. S. Weather Bureau, Washington, D. C., 1949, 287 pp.

8. Chandrashekhar Aiya, S. V., and B. S. Sondi, "Number of Cells Developed During the Life-time of a Thunderstorm," Nature, vol. 200, No. 4906, November 1963, pp 562-563.

9. Harper, W. G., and J. G. D. Beimers, "The Movement of Precipitation Belts as Observed by Radar," Quarterly Journal of the Royal Meteorological Society, vol. 84, No. 361, July 1958, pp. 242-249.

10. Hiser, H. W., and S. G. Bigler, "Wind Data from Radar Echoes," Technical Report No. 1, Illinois State Water Survey, Meteorological Laboratory, Urbana, Ill., March 1953, 18 pp.

11. Humphreys, W. J., Physics of the Air, 3d Ed., McGraw-Hill Book Co., New York, N. Y., 1940, 359 pp. (see pp. 353, 359).

12. Kessler, E., and J. A. Russo, Jr., "A Program for the Assembly and Display of Radar Echo Distributions," Journal of Applied Meteorology, vol. 2, No. 5, October 1963, pp. 582-593.

13. Ligda, M. G. H., "The Horizontal Motion of Small Precipitation Areas as Observed by Radar," Weather Radar Research, Technical Report No. 21, Massachusetts Institute of Technology, Cambridge, Mass., January 1953, 60 pp.

14. Ligda, M. G. H., and W. A. Mayhew, "On the Relationship Between the Velocities of Small Precipitation Areas and Geostrophic Winds," Journal of Meteorology, vol. 11, No. 5, October 1954, pp. 421-423.

15. Ligda, M. G. H., "Study of the Synoptic Application of Weather Radar Data," Final Report, Contract AF 19(604)-573, A. and M. College of Texas, 1956.

16. Ligda, M. G. H., "Middle Latitude Precipitation Patterns as Observed by Radar," Scientific Report No. 1, AFCRC-GRD Contract AF 19(604)-1564, A. & M. College of Texas, 1957.

17. Malkus, J. S., "Effects of Wind Shear on Some Aspects of Convection," Transactions of the American Geophysical Union, vol. 30, No. 1, February 1949, pp. 19-25.

18. Newton, C. W., and S. Katz, "Movement of Large Convective Rainstorms in Relation to Winds Aloft," Bulletin of the American Meteorological Society, vol. 39, No. 3, March 1958, pp. 129-136.

19. Newton, C. W., and H. R. Newton, "Dynamical Interactions Between Large Convective Clouds and Environment with Vertical Shear," Journal of Meteorology, vol. 16, No. 5, October 1959, pp. 483-496.

20. Staff Members, NSSP (National Severe Storms Project, U. S. Weather Bureau, Kansas City), "Severe Storm Detection and Circumnavigation," Final Report, FAA Contract ARDS-A-176, June 1963, Unit IV-A, 181 pp.

21. Workman, E. J., and S. E. Reynolds, "Time of Rise and Fall of Cumulus Cloud Tops," Bulletin of the American Meteorological Society, vol. 30, No. 10, December 1949, pp. 359-361.